UNITED NATIONS EDUCATIONAL, SCIENTIFIC AND CULTURAL ORGANIZATION
INTERNATIONAL ATOMIC ENERGY AGENCY
INTERNATIONAL CENTRE FOR THEORETICAL PHYSICS
I.C.T.P., P.O. BOX 586, 34100 TRIESTE, ITALY, CABLE: CENTRATOM TRIESTE

SMR: 962/5

WORKSHOP ON QUANTUM DISSIPATION AND APPLICATIONS

(29 July - 9 August 1996)

"Quantum Dissipation in Chemical and Biological Reactions" - II

presented by:

J.N. ONUCHIC
University of California at San Diego
Department of Physics
9500 Gilman Drive
La Jolla, CA 92095-0319
U.S.A.

Journal of Bioenergetics and Biomembranes, Vol. 27, No. 3, 1995

Pathways, Pathway Tubes, Pathway Docking, and Propagators in Electron Transfer Proteins

W. B. Curry,[1] M. D. Grabe,[1] I. V. Kurnikov,[1] S. S. Skourtis,[1] D. N. Beratan,[1] J. J. Regan,[2] A. J. A. Aquino,[2] P. Beroza,[2,3] and J. N. Onuchic[2]

Received February 28, 1995

The simplest views of long-range electron transfer utilize flat one-dimensional barrier tunneling models, neglecting structural details of the protein medium. The pathway model of protein electron transfer reintroduces structure by distinguishing between covalent bonds, hydrogen bonds, and van der Waals contacts. These three kinds of interactions in a tunneling pathway each have distinctive decay factors associated with them. The distribution and arrangement of these bonded and nonbonded contacts in a folded protein varies tremendously between structures, adding a richness to the tunneling problem that is absent in simpler views. We review the pathway model and the predictions that it makes for protein electron transfer rates in small proteins, docked proteins, and the photosynthetic reactions center. We also review the formulation of the protein electron transfer problem as an effective two-level system. New multi-pathway approaches and improved electronic Hamiltonians are described briefly as well.

KEY WORDS: Tunneling pathways; protein electron transfer; donor–acceptor interactions.

1. INTRODUCTION

Within a few picoseconds after absorbing light, photosynthetic organisms launch an electron down an efficient multi-step electron transfer chain (Feher *et al.*, 1989; Gunner, 1991). The ubiquitous single-electron transfer (ET) reaction lies at the center of cell metabolism as well. A sequence of one-electron oxidation–reduction reactions followed by proton transport generates a transmembrane electrochemical potential that energizes the synthesis of ATP. Recent developments in theoretical and experimental biophysical chemistry are beginning to indicate how proteins direct tunneling electrons to the right place at the right time (Lippard and Berg, 1994; Bertini *et al.*, 1994).

ET reactions occur throughout cell metabolism. Oxidases, peroxidases, oxygenases, hydrogenases, and nitrogenases perform key chemical transformations by the efficient coordinated transport of electrons. The enzyme nitrogenase, for example, makes ammonia from dinitrogen at atmospheric pressure and room temperature, a feat unequaled in the laboratory (Kim and Rees, 1994).

In the 1960's it was discovered that electron hops between redox groups in proteins are nonclassical (deVault, 1984). Electrons "tunnel" between spatially localized redox groups rather than being transported like delocalized electrons in metals (Hopfield, 1974). Since electron delivery to the wrong site can be lethal, quantum tunneling provides a likely means of controlling electron flow that is exquisitely sensitive to molecular architecture. Electron tunneling probabilities, zero for purely classical particles, drop roughly exponentially with distance. Recent studies indicate a richness in the mechanisms proteins might use to control electron tunneling rates. We will review some of the recent developments and challenges in this area.

[1] Department of Chemistry, University of Pittsburgh, Pittsburgh, Pennsylvania 15260.
[2] Department of Physics, University of California, San Diego, La Jolla, California 92093.
[3] Present address: Department of Molecular Biology, The Scripps Research Institute, La Jolla, California 92037.

0145-479X/95/0600-0285$07.50/0

2. PROTEINS: FORMLESS OR STRUCTURED TUNNELING BARRIERS?

Most biological electron transfer rates (k_{ET}) are described successfully with a nonadiabatic formulation because the donor–acceptor distance is large (and the interaction is weak) (Hopfield, 1974), so

$$k_{ET}(\vec{R}_{DA}) \propto (\text{electronic coupling})^2 (\text{nuclear factor}) \quad (1)$$

The nuclear factor is associated with the familiar activation barrier of Arrhenius theory (Sutin and Marcus, 1985; Marcus, 1993; Levich, 1965). The limits of validity for this rate expression have been discussed extensively (Onuchic *et al.*, 1986). This barrier arises because nuclei around the redox groups adjust their positions to accommodate the charge of the redox center. The electronic factor reflects how strongly the protein allows electron amplitude to leak across the protein from donor to acceptor. A detailed understanding of how proteins might control ET rates through this tiny quantum propagation proved elusive until recently.

Simple models of long-range electron transfer treat the protein between donor and acceptor as a one-dimensional square tunneling barrier (1DSB). As such, the rate is predicted to drop exponentially with distance (Hopfield, 1974; Jortner, 1976; Moser *et al.*, 1992; Beratan *et al.*, 1992a,b):

$$k_{ET}(\vec{R}_{DA}) \propto \exp[-\beta|\vec{R}_{DA}|](\text{nuclear factor}) \quad (2)$$

Far from the well, the probability of finding the particle drops exponentially, with a constant determined simply by the well depth, and this tunneling probability enters the ET rate directly. Accounting for the role of protein-mediated tunneling at this level of theory amounts to assigning a barrier height for tunneling. This barrier is associated with the energy difference associated with moving the electron from the donor to the surrounding protein. Hopfield's 1974 prediction ($\beta = 1.44$ Å^{-1}) stimulated numerous experiments on small molecule and macromolecule bridges of fixed length and known structure. *Rigid* bridges, keeping the donor–acceptor distance fixed, were built to test these ideas (see Bolton *et al.*, 1991, for example).

In the 1980's, a range of β values was observed for rigid electron transfer bridges. Theoretical analysis of these linkers predicts orbital energy and symmetry effects on the reaction rates. A fascinating balance of orbital interactions in model compounds seems to control the value of β, which varies with bridge structure (Bolton *et al.*, 1991; Closs and Miller, 1988; Wasielewski, 1992).

At the same time as intense work was being done on small molecules, a technology was developed to measure electron transfer rates in proteins between redox groups at fixed distance and orientation (Winkler and Gray, 1992; Therien *et al.*, 1991a,b). In proteins, just as in small molecules, donor and acceptor must be fixed in order for conclusions about bridge-mediated tunneling to be drawn unambiguously. A watershed in this field was the development of a new technology by Gray and co-workers to attach Ru complexes to proteins via surface histidines. This methodology, coupled with sophisticated electron-transfer kinetic experiments, provided the tools to probe the anisotropic nature of proteins as tunneling barriers (Therien *et al.*, 1990; Wuttke *et al.*, 1992; Karpishin, *et al.*, 1994).

Electron-transfer rates as a function of distance in model compounds and in proteins, when fitted to 1DSB models, produce a wide range of β values, ranging from 0.6 to 1.7 Å^{-1} (Mikkelson and Ratner, 1988; Therien *et al.*, 1991a,b). In small molecules, β values are consistently smaller than in proteins. This discrepancy provided the first experimental hint that the coupling mechanism in proteins might be qualitatively different from that in the smaller systems. The faster decay of rate with distance in proteins suggests that the coupling mechanism is less efficient. Looking at three-dimensional protein structures, a reasonable inference is that the mediation routes are less direct than in small molecule bridged systems.

In the late 1980's Onuchic and Beratan asked whether or not "measuring β" in proteins was a meaningful endeavor (Beratan *et al.*, 1987; Onuchic and Beratan, 1990). They argued that at physiological redox potentials *a single "universal" value of* β *does not exist.* The balance of through-bond and through-space contacts between donor and acceptor was proposed to set the coupling strength. They showed that mixing of the donor and acceptor states with the bonding orbitals of the bridge dominates the coupling process. This mechanism is referred to as "hole transfer." Their analysis suggested that ET rates in proteins should depend on the coupling pathway strength, rather than the linear distance between redox centers (Beratan *et al.*, 1991, 1992a,b).

3. TUNNELING PATHWAYS

What is the first step beyond a structureless tunneling barrier model of a protein? Electronic coupling

interactions mediated through bonds are longer range, in general, than interactions through space. Thus, it is convenient to break the electron tunneling into through-bond and through-space steps. The pathway strategy estimates the coupling as the product of decay factors along the most direct coupling route between donor and acceptor.

$$(\text{Electronic coupling}) \propto \Pi_i \epsilon_i^B \Pi_j \epsilon_j^H \Pi_k \epsilon_k^S \quad (3)$$

This expression represents a product of decay factors associated with each type of contact along a pathway (Beratan *et al.*, 1987; Onuchic and Beratan, 1990). Here the probability of tunneling between two points is determined by the *strongest coupling pathway* between those points. The through-bond decay parameters (B and H) are fixed at values estimated from model-compound experiments or from simple calculations. A critical aspect of the pathway model is the vital role of hydrogen bonds as tunneling mediators. Since the through-bond mechanism is dominated by hole transfer, hydrogen-bond mediation is particularly effective. The through-space decay factor is explicitly (and strongly!) distance dependent. Through-space decay is very costly; viable coupling pathways in proteins rarely contain more than one or two through-space steps. The strength of the strongest coupling pathways to a protein's surface from a redox center varies enormously (see Section 3.3). Pathways are easily identified using x-ray structural coordinates and a simple graph search algorithm (Betts *et al.*, 1992).

The pathway model has one essential feature built into it that is missing in 1DSB models. This is the radically different distance range for tunneling through a bonded medium and through empty space. The range of tunneling through space is set by the binding energy of the tunneling electron. An electron bound in a 1D well by 10 eV decays far from the well as $\exp(-1.7R)$ with R measured in Å. In contrast, the exponential decay constant associated with tunneling through covalent bonds and hydrogen bonds is *at least one-half of this value*. This intrinsic difference between through-bond and through-space tunneling defines the landscape for electron tunneling in proteins.

The sharp distinction between through-bond and through-space tunneling in proteins has at least two important and dramatic consequences. First of all, this line of analysis predicts that hydrogen bonds should be excellent tunneling mediators because they introduce relatively small through-space gaps between lone-pair electrons and $X - H$ bonds (Beratan *et al.*, 1987, 1991, 1992a,b; Onuchic and Beratan, 1990). This expectation was confirmed by experiments in Ru-modified proteins (Therien *et al.*, 1990, 1991a,b). In the absence of facile hydrogen bond-mediated tunneling pathways, electron-transfer rates should be orders of magnitude slower than what is actually observed. The second key prediction of the pathway model is that electrons tunnel very weakly across van der Waals gaps. This prediction was recently confirmed as well (Wuttke *et al.*, 1992).

Small redox proteins, like cytochrome *c*, contain a single redox center. The anisotropic structure of this protein is mirrored in the anisotropy of coupling pathways into the protein's redox center. A simple way of visualizing this anisotropy is to examine scatter plots of amino acid to redox-center coupling vs. amino acid to redox-center distance. 1DSB models put all of these points on a single exponential curve, whereas pathway models scatter these points orders of magnitude off of any single exponential curve (Beratan *et al.*, 1991, 1992a,b).

3.1. Functional Docking and ET

In many biological electron transfer reactions, an important ET step is *inter*molecular. However, theoretical work on electronic coupling in ET reactions has been confined largely to *intra*molecular ET. The intramolecular problem is simpler because the geometry is often relatively well known and the pathway analysis is straightforward.

The pathway model was recently extended to describe *inter*molecular electron transfer (Aquino *et al.*, 1995). This problem is particularly challenging because few electron transfer complexes have been subjected to detailed structural analysis. In existing x-ray structures, it is unclear whether or not the biologically relevant docking orientation is found in the solved structures. Furthermore, even if the interprotein docking orientation is known, the electron transfer rate is expected to be strongly dependent on the through-space decay associated with noncovalent contacts between molecules.

The interprotein pathway analysis strategy taken was to analyze couplings based on the *intra*molecular coupling in each interacting species. This allows the intermolecular through-space electron transfer, which is sensitive to the docking geometry, to be treated as a parameter to be analyzed. Thus, calculation of the coupling between the surface amino acids and the redox center permits a simple estimate of interprotein electronic coupling decay for a given docked structure.

The electronic coupling coupling is factored accordingly:

$$\text{(Electronic coupling)} \propto \Pi_i \epsilon_D(i) \Pi_j \epsilon_A(j) \epsilon_{\text{inter}} \quad (4)$$

where $\Pi_i \epsilon_D(i)$ is the electronic coupling decay between the electron donor site and the surface of the protein containing the electron donor; $\Pi_j \epsilon_A(j)$ is the electronic coupling decay between the electron acceptor site and the surface of the protein containing the acceptor; and ϵ_{inter} is the electronic coupling decay between protein surfaces (i.e., a through-space or hydrogen-bond coupling between surface atoms on the two proteins). Note that in Eq. (4) $\epsilon(i)$ and $\epsilon(j)$ can be any of the three types of decay (i.e., covalent, hydrogen-bonding, or through-space). Factoring the electronic coupling decay in this way separates quantities that are well defined, $\Pi_i \epsilon_D(i)$ and $\Pi_j \epsilon_A(j)$, from a quantity that is less well defined, ϵ_{inter}. The interprotein decay is poorly defined because the distance between proteins is not well established and geometrical changes from reference X-ray structures are not easily predicted.

A surface-to-redox center coupling map is obtained for each protein by calculating the electronic coupling decay, $|\Pi_i \epsilon(i)|^2$, between each surface atom and the redox center. These maps identify regions of the protein that can efficiently couple electron transfer from the redox site. Matching of strongly coupled regions on the two proteins will result in the maximal intermolecular electron transfer coupling (assuming ϵ_{inter} is not too small) and can be used as a criterion for evaluating putative docked structures. This criterion can supplement other criteria (e.g., electrostatic energy) for evaluating the overall functional importance of a docked structure.

Central to this strategy is the definition of protein surface. The main assumption is that an electron must proceed through a surface residue to leave the protein. We define a surface residue as one that is in contact with the molecular surface; the surface traced out as a spherical probe is rolled over the van der Waals surface of the protein. However, unlike the standard method, which uses a 1.4 Å radius spherical probe, we use a 3.0 Å radius probe. This generates a smoother surface and prevents atoms that border invaginations in the protein from being considered surface residues. This strategy is used because residues that line clefts in a protein are unlikely to be in contact with an atom on another protein in a docked structure.

From this analysis we can conclude that by generating surface coupling maps, we can learn a considerable amount about the coupling between proteins, but one still has to deal with the problem of the coupling between their surface residues. The functional docking strategy tells us which surface regions of the proteins one should put together in order to optimize the rate without addressing the question of docking stability. However, the length of the jump between the surface residues will be strongly dependent on the docking configuration, directly influencing the final coupling. Another important point to keep in mind is that all the calculations presented here have been performed for static structures. However, through-space jumps may be sensitive to dynamical motions. Increased attention to the dynamics of these contacts is certainly needed. The recent availability of x-ray crystal structures of docked electron transfer proteins is stimulating further work in this direction (Pelletier and Kraut, 1992; L. Chen *et al.*, 1994; Z. Chen *et al.*, 1994). Other studies are providing additional information about the dynamics of docking and ET as well (McLendon, 1991; Stemp and Hoffman, 1993).

3.2. Exponential and Nonexponential Distance Dependence in Biological ET

An essential feature of pathway analysis is the considerable scatter expected in log(rate) vs. distance plots (Beratan *et al.*, 1991, 1992a,b). This scatter was indeed seen in Ru protein systems. However, in the photosynthetic reaction center (PRC) of *Rps. viridis* (Deisenhofer and Michel, 1989), it was recently observed that scatter (correcting as well as possible for free energy and reorganization energy differences) is less pronounced (Moser *et al.*, 1992) than was found in the Ru-modified proteins.

We have calculated the tunneling pathway strengths in *Rps. viridis* (Fig. 1, Table I). Figure 2 shows a scatter plot of the pathway couplings squared (proportional to the ET rates after correction for free energy and reorganization energy differences (Moser *et al.*, 1992). A number of observations can be made that explain the lack of scatter in the rate data. The pathways possess two key features. First, the paths are "taut"; they fall nearly on a straight line of sight between the donor and acceptor pairs. Second, the early paths consist of limited through-space contacts (Table I). That is, the paths for the early reactions have similar through space-distances in the strongest paths. These paths are homologous to one another.

The later paths in the PRC (between quinones and from quinones back to the special pair) all have

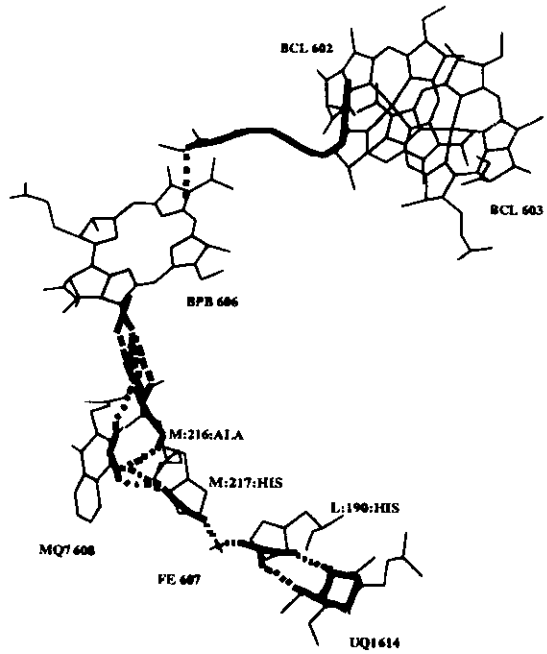

Fig. 1. Tunneling pathways (within 65% of the strongest) in the photosynthetic reaction center of *Rps. viridis* are shown for the forward ET reactions (see Table I).

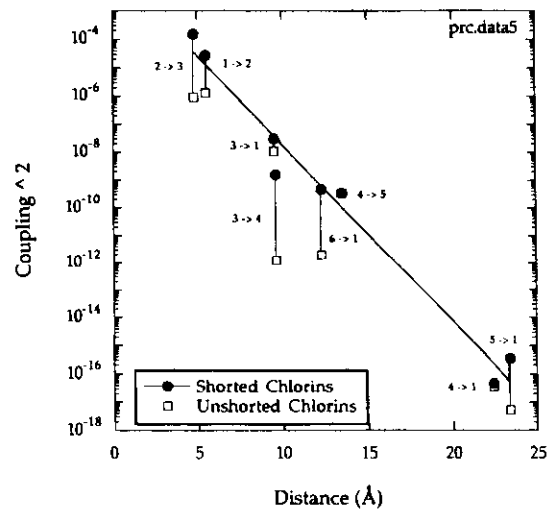

Fig. 2. Scatter plot of pathways couplings squared for charge separation and recombination pathways in the PRC. Solid dots are probably the most relevant calculation, corresponding to no penalty for tunneling across a chlorin ring (ring "shorting"). The best fit exponential to the solid dots is proportional to $e^{-1.47R}$, remarkably close to the experimental value (recall that the decay factors in the pathways method were taken to be as realistic as possible, based on model compound data and simple theoretical estimates). Rate nomenclature is given in Table I and in Moser *et al.*, 1992.

considerably longer nonbonded contacts than do the early reactions. The first ET reaction in the PRC competes with radiative decay to the ground state. The early charge shift steps compete with charge recombination. As such, smaller through-space distances in early pathways may be essential to overcome undesirable reactions. Through-space gaps in paths associated with later reactions are considerably larger. Such gaps presumably help to prolong the lifetime of the charge-separated states.

Is the decreased scatter of coupling in the PRC really a result of homologous pathways or related, in part, to the ET chromophores (chlorins and quinones)? A possible mechanism for decreasing scatter would arise from the integration of many pathways (each with a different strengths) by a large donor or acceptor. We have tested the idea of pathway integration in cytochrome *c* by averaging pathways to each surface atom within a region the size of a *second* heme on the protein's surface. We have averaged the absolute values of couplings within 4.6 Å of each surface atom (Fig. 3b) and compared them to the unprocessed coupling data (Fig. 3a). As such, we can determine whether docking a second large redox center would "average out" pathway effects. The degree of scatter in coupling vs. distance plots is not appreciably changed in this simple analysis. More complex analysis (e.g., adding random phase factors to the coupling data prior to summing and squaring) does not seem to decrease scatter either.

3.3. Single Paths, Multiple Paths, and Quantum Interference Between Pathways

The simple pathway product expression [Eq (3)] for electronic coupling suppresses quantum mechanical interference between pathways. A more general way of formulating the ET problem is to calculate the coupling as a function of a bridge "propagator" or Green's function that describes the electron mediation properties of the protein. In this case, the donor–acceptor coupling is

$$\text{(Electronic coupling)} \propto \text{(D to bridge coupling)} \times \text{(bridge propagator) (A to bridge coupling)} \quad (5)$$

Here no perturbation theory or pathway assumptions need to be made. Recently, there has been considerable interest in calculating and analyzing the protein propagator for a variety of Hamiltonians and at various levels

Table I. Tunneling Pathway Couplings in the Photosynthetic Reaction Center

D → A[a]	Coupling	Through-bond steps[b]	Hydrogen bonds	TS distances (Å)	Straight line distance (Å)[c]
1 → 2	5.286 E-03	3	0	3.28	5.5
2 → 3	1.235 E-02	4	0	2.48	4.8
3 → 4	3.999 E-05	7	1	3.44	9.6
4 → 5	1.839 E-05	12	0	7.20	13.5
3 → 1	1.728 E-04	10	0	3.19	9.5
4 → 1	6.911 E-09	17	1	8.63	22.4
5 → 1	1.832 E-08	16	0	8.66	23.4
6 → 1	2.148 E-05	11	1	2.79	12.3

[a] 1 = Special pair, 2 = chlorophyll (L), 3 = pheophytin (L), 4 = quinone A, 5 = quinone B, 6 = cytochrome.
[b] Number of covalent bonds in pathway.
[c] Shortest edge-to-edge distance.

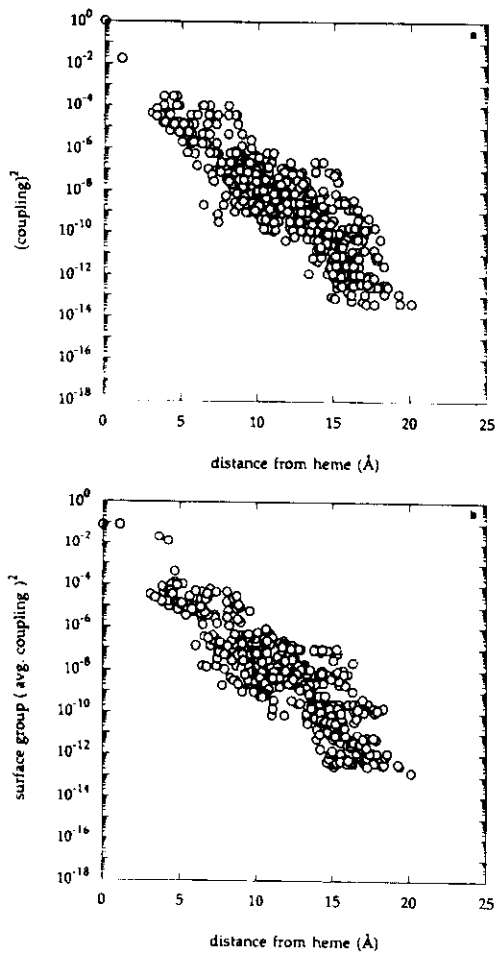

Fig. 3. (a) Standard scatter plot of coupling squared vs distance for cytochrome *c*. (b) Scatter plot of couplings squared for average coupling found within a 4.6 Å radius of each atom on the protein surface. Note that the degree of scatter is *not* decreased compared to (a).

of approximation (Regan *et al.*, 1993, 1995; Skourtis *et al.*, 1994; Gruschus and Kuki, 1993; Siddarth and Marcus, 1993). These methods capture, in principle, all multiple pathway and interference effects

There exists an infinite number of tunneling pathways that can be enumerated (including paths that retrace steps) in any protein. The electronic coupling can be written as a sum over contributions from these paths, and the summation should converge if the donor and acceptor states are sufficiently well localized:

$$(\text{Electronic coupling}) \propto \sum_{\text{paths}} \text{Coupling(path)} \quad (6)$$

Coupling pathways may interfere with one another constructively or destructively because this is a quantum problem. If multiple path effects are important, one anticipates that the secondary and tertiary folded motif, in addition to the strength of the largest coupling pathway, could be of importance in determining the electronic coupling. Recent work (Regan *et al.*, 1993, 1995) shows that interference effects can be divided into two classes and interpreted within the framework of pathway analysis. The first kind of interference arises from orbitals that interact strongly with the bonds on the dominant pathways (nearest neighbors and next nearest neighbors). This collection of paths creates a pathway family or tube that dominates the coupling in many cases. The interference of these similar paths with the main pathway is trivial in the sense that the single pathways can be viewed as simply having scaled parameters to account for these extra interactions. As different model compounds give rise to different β's, different secondary structures give rise to different types of pathway tubes.

The second type of pathway interference arises from interactions between distinct pathway tubes. Such

interactions are the subject of current investigation. Experiments have been performed to measure the rate of ET between the two metals in Ru-modified azurin (Langen *et al.*, 1995). Figure 4 shows a model of a section of azurin, highlighting the region between the copper and a $Ru(bpy)_2(im)$ probe bound to a histidine at position 83 (Day and Rees, 1995). In some experiments, the donor was placed on histidines on the 120's section of the protein chain, with a clear backbone pathway to the copper. This figure shows a contrasting case, where the placement of an acceptor at 83 provides no obviously dominant route between the metals. The intervening β-sheetlike structure, with its hydrogen bonds (shown as dashed lines), is a more complicated bridge than a simple backbone route. The "best path" apparently leaves the copper via 112 and takes a hydrogen bond (112:CYS:SG → 47:ASN:N-H) to get to 47, avoiding the long detour through the length of 46:HIS. It then takes one of two H bonds (48:TRP:N-HN → 84:THR:OG1, 48:TRP:O → 84:THR:N-HN) to get to the 80's section of the chain, to finally enter the HIS at 83, and thus the probe. Additional tubes are made possible by an H bond connecting the 120's chain to the 110's chain (121:MET:O → 112:CYS:N), and a second H bond connecting the 110's chain to the 40's chain (111:PHE:O → 49:VAL:N-HN). These alternative tubes all interfere with one another in the confluence of hydrogen bonds, and sum to give the resulting electronic coupling. The nature of this interference is not obvious; elimination of tubes by blocking certain H bonds in this structure can actually *increase* the coupling.

In addition to the work of Gray and co-workers, many others have provided considerable information about ET pathways in other proteins as well (Jacobs *et al.*, 1991; Sykes, 1991; Farver and Pecht, 1994; 1993; Moreira, 1994). A growing number of model compounds that contain biologically relevant bridging units, including hydrogen bonds and specific secondary motifs, is now being built as well (Anglos *et al.*, 1994; Ogawa *et al.*, 1993; Conrad *et al.*, 1992; Turro, 1993).

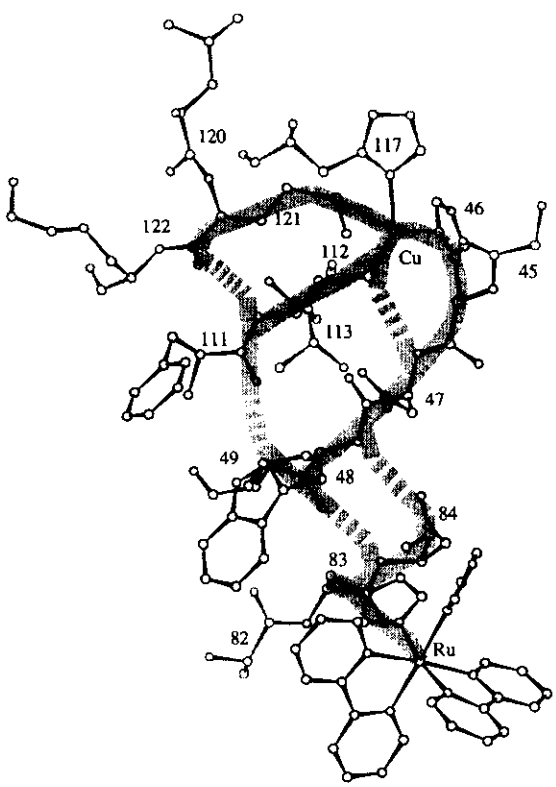

Fig. 4. Multiple pathway tubes traverse a β-sheet to provide the ET coupling from Cu to $Ru(bpy)_2(im)$(His 83) in modified azurin. Hydrogen bonds (dashed lines) are seen to play a crucial role in this coupling (Regan *et al.*, 1995).

4. TUNNELING ENERGIES AND THE TWO-LEVEL APPROXIMATION

A key assumption of nearly all ET rate theories is that the donor–protein–acceptor complex can be approximated as a two-level system (Larsson, 1981). That is, one assumes that the electron is well localized near the donor (acceptor) before (after) the electron transfer reaction. The validity of this approximation depends upon the size of the donor–acceptor interaction relative to the energy gap between donor/acceptor and mediating protein states (Skourtis and Onuchic, 1993; Skourtis *et al.*, 1993).

In the protein ET problem the donor–acceptor interaction is much smaller than the energy gap (ratio of about 10^{-6}), and the two-state approximation is valid. For the primary charge separation reaction in the PRC (and for some small molecule ET compounds) intermediate bridge states may be strongly coupled to donor and acceptor, rendering this approximation invalid. In such cases, it is still possible to describe the ET process in terms of pathways (Hu and Mukamel, 1989; Skourtis and Mukamel, 1995). It is, however, necessary to distinguish between pathways that visit the population of the intermediate bridge states (sequential mechanism) from pathways that do not (superexchange mechanism).

5. QUANTUM CHEMICAL CALCULATIONS OF ELECTRON TUNNELING IN PROTEINS

Electronic coupling can, in principle, be calculated by solving the Schrödinger equation for a molecular electronic wave function of the donor, acceptor, and intervening protein system using techniques of quantum chemistry. While accurate *ab initio* methods (Szabo, 1989) have been rather successfully applied to study electronic coupling in small model compounds (Jordan and Paddon-Row, 1992; Shephard *et al.*, 1993; Curtiss *et al.* 1993; Newton, 1991), it is not possible currently to implement these methods for proteins because the required computational time grows very rapidly with the size of the system.

Existing semiempirical quantum chemical methods (like extended Hückel) technically permit the study of systems with several hundreds of atoms, and have been applied to calculate electronic couplings in proteins (Broo and Larsson, 1991; Siddarth and Marcus, 1993; Regan *et al.*, 1993). These simple methods do involve some adjustable parameters which were originally set to reproduce heats of formation and optical transition energies of chemical compounds (ground and excited electronic state properties of the neutral systems).

The electronic propagator mentioned in Section 3.3 [Eq (5)] describes the coupling mediated by the protein. This propagator depends on properties of electronic states of the system with one extra electron added (N + 1 electron states), one electron removed (N − 1 electron states), and on the transitions energies between the ground (N electron) state and the N + 1 and N − 1 electron states (i.e., electron affinities and ionization potentials, respectively). Thus, we expect that standard semiempirical methods will be of limited use for proteins and entirely new parameter sets must be developed that properly reproduce these quantities. One attempt of this kind was reported by Gruschus and Kuki (Gruschus and Kuki, 1993). The authors developed a simple Hamiltonian for electronic coupling in proteins based upon tailored site energies that neglected some of the chemical features of the amino acids but reproduced experimental ionization potentials for amino acids and built the intersite interactions to be consistent with *ab initio* calculations on model compounds.

We are currently parametrizing an extended Hückel-like Hamiltonian to study ET in proteins based upon accurate *ab initio* calculations of the electron propagator matrices of amino acids. This new method works well on model ET compounds, and we hope that it will provide an improved quantitative description of ET coupling in proteins (Kurnikov and Beratan, 1995).

6. CONCLUSIONS

In summary, theory and experiment are in agreement that protein structure can be used for gross (distance) and fine (pathway) control of ET rates. In some proteins, the anisotropy of the paths emanating from a redox center is very large indeed. However, in specific redox reactions, the anisotropy may be less apparent because pathways between centers sample very special subregions of the protein. This may be the case in the photosynthetic reaction center. The tunneling pathway model succeeds because it correctly captures the distinct difference between electron propagation through bond (including hydrogen bonds) and through space. ET rates in Ru-labeled cytochromes *c* that are inconsistent with 1DSB models are understood in the context of the pathway model. Quantum interference between pathways is the subject of current theoretical (Regan *et al.*, 1995; Skourtis *et al.*, 1995) and experimental investigation, and these studies should lead to a deeper understanding of protein-mediated redox chemistry. Current research is also progressing toward more reliable Hamiltonians, and that should allow one to address detailed chemical questions about energetics, symmetry, and bonding in the mediation of long-range electron transport (Regan *et al.*, 1995; Kurnikov and Beratan, 1995). Stimulated by recent experiments, theoretical studies are now being aimed at ET in docked interprotein complexes as well.

ACKNOWLEDGMENTS

This work is supported by the National Science Foundation (CHE-9257093 and MCD-9316186), the National Institutes of Health (GM48043-2), and the Department of Energy (DE-FG36-94G010051).

REFERENCES

Anglos, D., Bindra, V., and Kuki, A. (1994). *J. Chem. Soc. Chem. Comm.* 213–215.

Aquino, A. J. A., Beroza, P., Beratan, D. N., and Onuchic, J. N. (1995). *Chem. Phys.*, in press.

Beratan, D. N., Betts, J. N., and Onuchic, J. N. (1992b). *J. Phys. Chem.* **96**, 2852–2855.
Beratan, D. N., Betts, J. N., and Onuchic, J. N. (1991). *Science* **252**, 1285–1288.
Beratan, D. N., Onuchic, J. N., and Hopfield, J. J. (1987). *J. Chem. Phys.* **86**, 4488–4498.
Beratan, D. N., Onuchic, J. N., Winkler, J. R., and Gray, H. B. (1992a). *Science* **258**, 1740–1741.
Bertini, I., Gray, H. B., Lippard, S., and Valentine, J. (1994). *Bioinorganic Chemistry*, University Science Books, Mill Valley, CA.
Betts, J. N., Beratan, D. N., and Onuchic, J. N. (1992). *J. Am. Chem. Soc.* **114**, 4043–4046.
Bolton, J. R., Mataga, N., and McLendon, G. (1991). *Electron Transfer in Inorganic, Organic, and Biological Systems, Advances in Chemistry Series 228*, ACS Press, Washington, DC.
Broo, A., and Larsson, S. (1991). *J. Phys. Chem.* **95**, 4925–4928.
Chen, L., Durley, R., Mathews, F., and Davidson, V. (1994). *Science* **264**, 86–90.
Chen, Z., Koh, M., Vandriessche, G., Vanbeeumen, J., Bartsch, R., Meyer, T., Cusanovich, M., and Matthews, F. (1994). *Science* **266**, 430–432.
Closs, G., and Miller, J. R. (1988). *Science* **240**, 440–447.
Conrad, D. W., Zhang, H., Stewart, D. E., and Scott, R. A. (1992). *J. Am. Chem. Soc.* **114**, 9909–9915.
Curtiss, L. A., Naleway, C., and Miller, J. (1993). *Chem. Phys.* **176**, 387–405.
Day, M., and Rees, D. C. (1995). Private communication.
Deisenhofer, J., and Michel, H. (1989). *Science* **245**, 1463–1473.
de Vault, D. (1984). *Quantum Mechanical Tunneling in Biological Systems, 2nd edition.* Cambridge Press.
Farver, O., and Pecht, I. (1994). *Biophys. Chem.* **50**, 203–216.
Feher, G., Allen, J., Okamura, M., and Rees, D. (1989). *Nature* **339**, 111–116.
Gruschus, J. M., and Kuki, A. (1993). *J. Phys. Chem.* **97**, 5581–5593.
Gunner, M. (1991). *Curr. Topics Bioenerg.* **16**, 319–367.
Hopfield, J. J. (1974). *Proc. Natl. Acad. Sci. (USA)* **71**, 3640–3644.
Hu, Y., and Mukamel, S. (1989). *J. Chem. Phys.* **91**, 6973–6988; *Chem. Phys. Lett.* **160**, 410–416.
Jacobs, B. A., Mauk, M., Funk, W., MacGillivray, R., Mauk, A. G., and Gray, H. B. (1991). *J. Am. Chem. Soc.* **113**, 4390–4394.
Jordan, K. D., and Paddon-Row, M. N. (1992). *Chem. Rev.* 395–410.
Jortner, J. (1976). *J. Chem. Phys.* **64**, 4860–4867.
Karpishin, T. B., Grinstaff, M., Komar-Panicucci, S., McLendon, G., Gray, H. B. (1994). *Structure* **2**, 415–422.
Kim, J., and Rees, D. C. (1994). *Biochemistry* **33**, 389–397.
Kurnikov, I. V., and Beratan, D. N. (1995). In preparation.
Langen, R., Chang, I. J., Germanas, J. P., Richards, J. H., Winkler, J. R., and Gray, H. B. (1995). *Science* **268**, 1733–1735.
Larsson, S. (1981). *J. Am. Chem. Soc.* **103**, 4034–4040.
Levich, V. G. (1965). In *Advances in Electrochemistry and Electrochemical Engineering* (Delahay, P., and Tobias, C. W., eds.) Interscience. New York, Vol. 4, pp. 249–372.
Lippard, S. J., and Berg, J. M. (1994). *Principles of Bioinorganic Chemistry*, University Science Books, Mill Valley, CA.
Marcus, R. A. (1993). *Angew. Chemie., Int. Ed. Engl.* **32**, 1111–1121.
McLendon, G. (1990). *Structure and Bonding* **75**, 159–174.
Mikkelson, K. V., and Ratner, M. A. (1988). *Chem. Rev.* **87**, 113–153.
Moreira, I., Sun, J., Cho, M., Wishart, J., and Isied, S. (1994). *J. Am. Chem. Soc.* **116**, 8396–8397.
Moser, C. C., Keske, J. M., Warncke, K., Farid, R. S., and Dutton, P. L. (1992). *Nature* **355**, 796–802.
Newton, M. D. (1991). *Chem. Rev.* **91**, 767–792.
Ogawa, M. Y., Wishart, J., Young, Z., Miller, J., and Isied, S. (1993). *J. Phys. Chem.* **97**, 11456–11463.
Onuchic, J. N., and Beratan, D. N. (1990). *J. Chem. Phys.* **92**, 722–733.
Onuchic, J. N., Beratan, D. N., and Hopfield, J. J. (1986). *J. Phys. Chem.* **90**, 3707–3721.
Onuchic, J. N., Beratan, D. N., Winkler, J. R., and Gray, H. B. (1992). *Ann. Revs. Biophys. Biomol. Struct.* **21**, 349–377.
Pelletier, H., and Kraut, J. (1992). *Science* **258**, 1748–1755.
Regan, J. J., DiBilio, A. J., Langen, R., Skov, L. K., Winkler, J. R., Gray, H. B., and Onuchic, J. N. (1995). Chemistry and Biology, in press.
Regan, J. J., Risser, S. M., Beratan, D. N., and Onuchic, J. N. (1993). *J. Phys. Chem.* **97**, 13083–13088.
Shephard, M. J., Paddon-Row, M. N., and Jordan, K. D. (1993). *Chem. Phys.* **176**, 289–304.
Siddarth, P., and Marcus, R. A. (1993). *J. Phys. Chem.* **97**, 13078–13082.
Skourtis, S. S., Beratan, D. N., and Onuchic, J. N. (1993). *Chem. Phys.* **176**, 501–520.
Skourtis, S. S., Beratan, D. N., and Onuchic, J. N. (1995). *Inorg. Chim. Acta*, submitted.
Skourtis, S. S., and Mukamel, S. (1995). *Chem. Phys.*, in press.
Skourtis, S. S., Regan, J. J., and Onuchic, J. N. (1994). *J. Phys. Chem.* **98**, 3379–3388.
Skourtis, S. S., and Onuchic, J. N. (1993). *Chem. Phys. Lett.* **209**, 171–177.
Stemp, E. D. A., and Hoffman, B. M. (1993). *Biochemistry* **32**, 10848–10865.
Sutin, N., and Marcus, R. A. (1985). *Biochim. Biophys. Acta* **811**, 265–322.
Sykes, A. G. (1991). In *Electron Transfer Reactions in Metalloproteins, Vol. 27* (Sigel, H., and Sigel, A., eds.). Marcel Dekker, New York, pp. 291–321.
Szabo, A. (1989). *Modern Quantum Chemistry, Revised First Edition.* Macmillan, New York.
Therien, M. J., Bowler, B. E., Selman, M. A., Gray, H. B., Chang, I. J., and Winkler, J. R. (1991). In *Electron Transfer in Inorganic, Organic, and Biological Systems, Advances in Chemistry Series 228*, ACS Press, Washington, DC, pp. 191–199.
Therien, M. J., Chang, J., Raphael, A. L., Bowler, B. E., and Gray, H. B. (1991). *Structure and Bonding* **75**, 109–129.
Therien, M. J., Selman, M., Gray, H. B., Chang, I. J., and Winkler, J. R. (1990). *J. Am. Chem. Soc.* **112**, 2420–2422.
Turro, C., Chang, C., Leroi, G., Cukier, R., and Nocera, D. (1992). *J. Am. Chem. Soc.* **114**, 4013–4015.
Wasielewski, M. R. (1992). *Chem. Rev.* **92**, 435–461.
Winkler, J. R., and Gray, H. B. (1992). *Chem. Rev.* **92**, 369–379.
Wuttke, D. S., Bjerrum, M. J., Winkler, J. R., and Gray, H. B. (1992). *Science* **256**, 1007–1009.

Reprinted from The Journal of Physical Chemistry, 1988, 92, 6495.

Classical and Quantum Pictures of Reaction Dynamics in Condensed Matter: Resonances, Dephasing, and All That

José Nelson Onuchic[†,§] and Peter G. Wolynes*[,‡,§,⊥]

Instituto de Fisica e Quimica de Sao Carlos, Universidade de Sao Paulo, 13560, Sao Carlos, SP, Brazil; Noyes Laboratory, University of Illinois, Urbana, Illinois 61801; Institute for Theoretical Physics, University of California, Santa Barbara, California 93106; and Institute for Molecular Science, Okazaki, 444 Japan
(Received: April 26, 1988)

A remarkably rich picture of the dynamics of chemical reactions in condensed-phase systems has emerged in recent years. The interplay of friction, electronic nonadiabaticity, and intramolecular energy flow have been elucidated by use of pictures based on classical trajectories. We review the qualitative ideas of that picture. There are some significant limitations of that approach to reaction dynamics that arise from quantum interference effects. Using a trajectory picture along with the quantum superposition principle, we give qualitative arguments describing how the transmission coefficient for nonadiabatic barrier crossing can be affected by resonances. We highlight the connections and differences between classical friction and quantum mechanical dephasing effects in barrier crossing. We also discuss the relation of this trajectory-based picture and the traditional language of radiationless processes based on the Golden Rule and master equations.

I. Introduction

Remarkable progress toward the goal of being able to visualize the progress of condensed-phase reactions in terms of the details of molecular motion has been made in the past decade. Besides the aesthetic motivation for pursuing this goal, it has become apparent that the deeper understanding reveals new aspects of the control of chemical reaction rates by the molecular environment. An example of this is the emerging picture of the interplay between molecular dynamical control (see ref 1–10, for example) and electronic control (see ref 11–20) in electron-transfer and biomolecular reactions.

Most of this progress in reaction theory has been based on classical or semiclassical descriptions of molecular motion.[21] Although tunneling[22] has received a good deal of attention, other fundamentally quantum mechanical aspects of molecular motion have not been closely examined for reaction dynamics in condensed phases. For example, the fact that quantum dynamics is described by probability amplitudes which can constructively or destructively interfere has not figured in most descriptions of reaction dynamics in condensed matter. These interference effects, which can persist at high temperatures, are known to be important in gas-phase chemical reactions.[23,24] They are responsible for the resonances in the prototypical $H_2 + F$ reaction. The possibility that interference effects and resonances occur has also been raised in the context of biomolecular reactions.[25] The existence and tuning of resonances have been speculatively introduced as a control mechanism in biomolecular systems.

Quantum interference effects require the preservation of phase relationships. In the condensed phase, we now know[26] that there are a variety of mechanisms for destroying phase relationships and these are intimately related to molecular motion. This has been most dramatically revealed by the recent experimental advances in nonlinear spectroscopy. One of the early surprises coming from that field was the occasional disparity of time scales between these dephasing processes and processes leading to energy flow (another feature of molecular motion). A careful examination of these quantum interference effects and their destruction by the molecular environment therefore seems worthwhile.

In this paper we will discuss how these quantum dynamic effects can be included in a nearly classical picture of molecular motion in barrier-crossing events. We will focus on the issue especially

* To whom correspondence should be addressed at the University of Illinois.
† Universidado de Sao Paulo.
‡ University of Illinois.
§ University of California.
⊥ Institute for Molecular Science.

(1) *Protein, Structure, Molecular and Electronic Reactivity*; Austin, R., Buhks, E., Chance, B., Devault, D., Dutton, P. L., Frauenfelder, H., Gol'danskii, V. I., Eds.; Springer-Verlag: New York, 1987.
(2) Newton, M. D.; Sutin, N. *Annu. Rev. Phys. Chem.* **1985**, *35*, 437.
(3) Marcus, R. A.; Sutin, N. *Biochim. Biophys. Acta* **1985**, *811*, 265.
(4) Frauenfelder, H.; Wolynes, P. G. *Science* **1985**, *229*, 337.
(5) Garg, A.; Onuchic, J. N.; Ambegaokar, V. *J. Chem. Phys.* **1985**, *83*, 4491.
(6) Hopfield, J. J. *Proc. Natl. Acad. Sci. U.S.A.* **1974**, *7*, 3640.
(7) Goldstein, R. F.; Bialek, W. *Phys. Rev. B: Condens. Matter* **1983**, *27*, 7431.
(8) Jortner, J. *Biochim. Biophys. Acta* **1980**, *594*, 193.
(9) Zusman, L. D. *Chem. Phys.* **1980**, *49*, 259.
(10) Wolynes, P. G. *J. Chem. Phys.* **1987**, *86*, 1957.
(11) Redi, M.; Hopfield, J. J. *J. Chem. Phys.* **1980**, *72*, 6651.
(12) Beratan, D. N.; Hopfield, J. J. *J. Am. Chem. Soc.* **1984**, *106*, 1584.
(13) Onuchic, J. N.; Beratan, D. N. *J. Am. Chem. Soc.* **1987**, *109*, 6771.
(14) Onuchic, J. N.; Beratan, D. N.; Hopfield, J. J. *J. Phys. Chem.* **1986**, *90*, 3707.
(15) da Gama, A. A. S. *Theor. Chim. Acta* **1985**, *68*, 159.
(16) Siders, P.; Cave, R. J.; Marcus, R. A. *J. Chem. Phys.* **1984**, *81*, 5613.
(17) Hale, P. D.; Ratner, M. A. *Int. J. Quantum Chem., Quantum Chem. Symp.* **1984**, *18*, 195.
(18) Logan, J.; Newton, M. D. *J. Chem. Phys.* **1983**, *78*, 4086.
(19) Beratan, D. N.; Onuchic, J. N.; Hopfield, J. J. *J. Chem. Phys.* **1987**, *86*, 4488.
(20) Kuki, A.; Wolynes, P. G. *Science* **1987**, *236*, 1647.
(21) In addition to the references cited above, see for a review: Truhlar, D. G.; Hase, W. L.; Hynes, J. T. *J. Phys. Chem.* **1983**, *87*, 2664.
(22) In addition to the references cited above, see for a review: Hanggi, P. *J. Stat. Phys.* **1985**, *42*, 105. Addendum and erratum: *Ibid.* **1986**, *44*, 1003.
(23) "Molecular Scattering: Physical and Chemical Applications", *Advances in Chemical Physics*; Lawey, K. P., Ed.; Wiley: London, 1975.
(24) Lee, W. T. *Physics of Electronic and Atomic Collisions*, VII ICPEAC; North-Holland: Amsterdam, 1971; p 357.
(25) (a) Bialek, W.; Goldstein, R. F. *Phys. Scr.* **1986**, *34*, 273. (b) Friesner, R.; Wertheimer, R. *Proc. Natl. Acad. Sci. U.S.A.* **1982**, *79*, 2138.
(26) *Radiationless Processes in Molecules and Condensed Phases*; Fong, F. K., Ed.; Springer-Verlag: New York, 1976. See especially the article by K. Freed.

for nonadiabatic processes, like electron transfer where the issue of electronic versus dynamic control is central. The nature of much of the discussion is semiquantitative, dimensional arguments which should act as an orientation to future analytic or computational approaches. We will first review the classical and semiclassical pictures of molecular dynamic effects on barrier crossing. In doing so, we take the opportunity to comment on some open questions in modeling chemical reactions in condensed phases. Then we will include interference and dephasing effects in these trajectory arguments. Following this we will show the close connection of these ideas with approaches based on master equation descriptions using Golden Rule arguments[27,28] and energy relaxation arguments.[26] This latter approach is familiar in the radiationless transition literature. Those familiar with that literature will not be surprised by the results of the earlier arguments, but we feel there is novelty and pedagogical value in presenting the former approach because of its similarity to the work on purely classical barrier-crossing processes. Finally, we will indulge in a speculation on extensions, experimental tests, and applications of these ideas.

II. Classical and "Completely" Semiclassical Arguments for Barrier Crossing

The kinetic significance of explicitly quantum mechanical effects, such as tunneling and curve crossing, on rate coefficients has long been appreciated. That the details of molecular motion are also relevant was recognized early[29] but, in the context of condensed-phase reactions, largely ignored until the past decade.[21] Still more recent is the widespread realization that these features are coupled.[22] In the following subsections, we will review some of the simple arguments in this area. This covers much the same ground as the paper of Frauenfelder and Wolynes, albeit more briskly and a bit more technically.[4]

II.a. Classical Barrier Crossing. The transition-state theory of classical barrier crossing finesses beautifully the question of molecular dynamics.[30,31] It does so by replacing the question, How many reactive events occur per unit time? by the question, At equilibrium, how many crossings from reactant to product occur? After the choice of a definition of reactant and product (through a prescription for a dividing surface in phase space), the latter question can be answered by equilibrium statistical mechanics. It is simply the number of systems at the dividing surface, which is given by the Boltzmann distribution, times the velocity-weighted fraction moving toward product.

From the above verbal description it follows that the transmission coefficient $\kappa = k/k_{TST}$ can be estimated as the inverse of the typical number of forward crossings per reactive event. Said another way, transition-state theory has counted each of the forward crossings in a single reactive event as a completed reaction and so this overcounting must be corrected for.[32]

Clearly, the interplay between molecular motion and chemical reaction outlined above depends on both the objective dynamics of the system and the subjective choice of the dividing surface and the corresponding reaction coordinate, which at the transition state is orthogonal to it. If we wish to use our intuition about molecular motion to understand the reaction dynamics, we will likely choose reaction coordinates that correspond with some aspect of single-molecule motion, such as an internal bond rotation, or, perhaps, some simple collective coordinate, such as the electrical polarization of the medium. Having just said this, we should not be blinded to the possibility that carefully chosen reaction coordinates may obviate, at least partially, the need to carry out a detailed study of the dynamics.

Molecular motions are often described with the concept of "friction". The reaction coordinate, through its interactions with the other degrees of freedom of the system, suffers changes in velocity and energy. Mathematically, friction on the reaction coordinate has been described in a few ways. One of the most popular is the Langevin equation and its generalization.[33] Here the motion of the reaction coordinate is described by a stochastic process in which Newton's laws are modified through the addition of a frequency-dependent but linear friction force and a Gaussianly distributed random force. Another popular way to describe the reaction coordinate motion is to imagine its Newtonian motion as being interrupted occasionally by "collisions" which modify the velocity and energy of the coordinate in a random fashion.[34,35] Both of these pictures are used primarily to describe molecular motion in a liquidlike environment.

The exact limits of the Langevin description have not been entirely proscribed. Generally, we expect it to be valid when at any time the reaction coordinate is coupled to many other degrees of freedom, in each case, however, weakly. That is, it can arise from a dynamic central limit theorem. Alternatively, if the other degrees of freedom are truly harmonic and thereby Gaussianly distributed, such a description should be valid. The fact that a generalized Langevin description is equivalent to an *effective* set of oscillators is very useful in transcribing results to quantum mechanics.

The "collision" picture is valid even if the degrees of freedom of the bath interact strongly, but the interaction must be brief relative to the interval between such interactions and be brief relative to the natural time scales of the reaction coordinate motion. The two pictures, Langevin and collision, merge for the case of Fokker–Planck friction in which the collisions are frequent but very weak.[34]

These two ways of describing friction are by no means exhaustive. The study of molecular motion in condensed phases is far from being completed. At least two important exceptions to these pictures will play a role in the study of chemical kinetics in condensed phase. In extremely sluggish media, such as very viscous fluids or glasses, the large friction is apparently due to some sort of activated processes.[36-38] These processes are not likely to be described by simple Langevin theory or by a collision theory. Since, as we shall see, the limit of large friction is important, this lacuna in our understanding is quite important. Another exception of importance will be those cases where the reaction coordinate interacts with a few other degrees of freedom with similar vibrational time scales. Here one has the possibility of *nonlinear* resonances and, as we know, the phenomena of dynamical chaos and intermittency. Since energy flow in small molecules in solids involves such mechanisms,[39] we must be careful to be sure, when using the results of Langevin or collision pictures, that only their most general features are entering into the prediction.

In most of the ways of describing friction, classically, a crucial role is played by the velocity relaxation time τ_v and the corresponding mean free path $l = v\tau_v$. If l is much shorter than the other relevant length scales, the motion is essentially diffusive, like a random walker with a step length l, irrespective of the underlying model. On the other hand, if l is long, compared to other length scales, or equivalently τ_v long compared to other time scales, details of the friction do matter.

Armed with these notions, we can describe some simple behaviors for the transmission coefficient for classical barrier crossing. Within these pictures, the simplest case is the high-friction, diffusive regime. Here a purely configurational view of the dividing surface and the transition-state region is appropriate. Once a system on a trajectory has an energy lower than the barrier height by about k_BT, it will typically settle into whichever side of the well it is on at the time. We can call the corresponding

(27) Jortner, J. *Philos. Mag. B* **1979**, *41*, 317.
(28) Holstein, T. *Philos. Mag. B* **1978**, *37*, 499.
(29) Kramers, H. A. *Physica* **1940**, *7*, 284.
(30) Wigner, E. *J. Chem. Phys.* **1937**, *5*, 720.
(31) Eyring, H. *J. Chem. Phys.* **1934**, *3*, 107.
(32) Keck, J. C. *Adv. Chem. Phys.* **1967**, *13*, 85.
(33) See: Adelman, S. *Adv. Chem. Phys.* **1980**, *44*, 143.
(34) Skinner, J. L.; Wolynes, P. G. *J. Chem. Phys.* **1978**, *69*, 2143 **1980**, *72*, 4913.
(35) Montgomery, J. R.; Chandler, D.; Berne, B. J. *J. Chem. Phys.* **1978**, *70*, 4065.
(36) Zwanzig, R. *J. Chem. Phys.* **1963**, *38*, 1603.
(37) Weber, T.; Stillinger, F. *Phys. Rev. B: Condens. Matter* **1985**, *31*, 1954; *Phys. Rev. A* **1983**, *28*, 2408.
(38) Hall, R.; Wolynes, P. G. *J. Chem. Phys.* **1987**, *86*, 2943.
(39) Bondybey, V. *Annu. Rev. Phys. Chem.* **1984**, *35*, 591.

distance in the reaction coordinate from the transition state l_{TST}. Once the system has diffused this distance, it is trapped in one of the wells. The total number of steps taken in the transition-state region is of order $(l_{TST}/l)^2$ by using the well-known relation for random walks. The number of recrossings is the fraction of these steps occurring over the saddle point itself. Since a step is of length l, this fraction is l/l_{TST} and, therefore, the number of recrossings is l_{TST}/l. The transmission coefficient is hence proportional to the mean free path and is $\kappa = l/l_{TST}$. In this regime the rate is inversely proportional to the friction and proportional to the diffusion constant.

The result for the high-friction regime, sometimes known as the Smoluchowskii or somewhat improperly Kramers regime, would seem quite robust, from the above argument. In fact, deviations are often observed. These are due to a breakdown of the random walk picture. If friction is increased by going to more viscous solvents, the change in friction largely comes from a change in time scale of the viscoelastic response of the medium. The random walk becomes correlated and is not described by a single mean free path. Using a Langevin description of the friction, Grote and Hynes have shown how an effective friction at the time scale of transition-state motion enters in this case.[40] That is, diffusion arguments apply with a mean free path relevant to the short time it takes to cross the transition region. This is a beautiful and important result. We should bear in mind, however, that it is also in this regime that the Langevin picture may break down. One way to achieve the diffusive limit is to ensure that the reaction coordinate corresponds with the motion of a bulky rigid object in a moderately viscous medium. In this hydrodynamic limit, the diffusive picture is generally confirmed.[41,42]

The diffusive limit with its Grote–Hynes amplification has an amusing aspect.[43] If the Langevin picture is used, as we have said, the other degrees of freedom can be modeled *effectively* as harmonic degrees of freedom. If the many-dimensional coupled system of these effective degrees of freedom with the reaction coordinate is treated by transition-state theory, one obtains the Grote–Hynes result. Does this mean the Grote–Hynes or diffusive result is just transition-state theory? Not at all! Of course, if the effective harmonic bath is identical with the real bath as may happen in a crystalline solid, it is. However, the Langevin forces in the fluid state, if validly described that way, come from the central limit theorem mechanism. The effective degrees of freedom are only marginally related to the original degrees of freedom in the problem. We have no guarantee that transition-state theory in the original multidimensional system will give the correct result.

The region of low damping, i.e., long mean free path, is also interesting. Here the details of energy flow into and out of the reaction coordinate matter.[34,44,45] The number of recrossings will depend on the time it takes the reaction coordinate to lose at least k_BT of energy, τ_e, and on the rate of making recrossings for such an activated molecule, k_E:

$$N_c \approx \tau_E k_E \tag{2.1}$$

Notice this estimate assumes that recrossing is a Markovian process with no intermittency. This ansatz may well fail when flow of energy from the reaction coordinate to other internal modes of motion is concerned. Nevertheless, it is useful in two limits: (1) no flow to other modes and (2) extremely rapid flow to other modes—the RRKM limit.[44,45] Let us first estimate the time τ_E in the one-dimensional case. This depends on the model for the friction. For Langevin (i.e., Fokker–Planck) friction the energy loss rate is equal to the power dissipated against the frictional force. The power is given in terms of the velocity v. $P = \zeta v^2$ where the average is taken over a cycle of motion. If the frequency dependence of the friction is large, then ζ should be taken to be $\zeta(\Omega_0)$ where Ω_0 is the vibration frequency in the well. The average of v^2 over a cycle of harmonic motion is $E^\ddagger/M$ based on the virial theorem ($E^\ddagger$ is the activation barrier) and the fact that crossing trajectories must have energy near the barrier height.

Thus, we see that

$$\tau_E = k_BT/P = \frac{k_BT}{E^\ddagger}\frac{M}{\zeta} = \frac{k_BT}{E^\ddagger}\tau_v \tag{2.2}$$

As the barrier gets higher, this time gets shorter since energy is rapidly dissipated. On the other hand, for a stronger collision picture, such as the BGK model in which thermalization is complete upon a single collision, the relevant relation of τ_v and τ_E is different. For the BGK collision model $\tau_E = \tau_v$. For Lorentz models, in which the reaction coordinate is a light degree of freedom and the bath is heavy, τ_E can be much greater than τ_v; i.e., the direction of motion is randomized more rapidly than the speed of motion.

For the one-dimensional case (i.e., no energy flow to other internal modes) the rate of making crossings is just the vibrational frequency $\Omega_0/2\pi$. (Here we have made the assumption that both surfaces, reactant and product, are harmonic with frequency Ω_0.) Thus, in this regime, the number of recrossings inversely proportional to the friction and the transmission coefficient is proportional to the friction or collision rate. This is the regime in which obtaining the energy of activation is the rate-determining step, just as in the classical Lindemann picture for gas-phase reactions.

What happens in the case of rapid internal energy flow? Depending on the collisional model τ_E may change. The energy will be shared among all the modes equally (for a classical model). For Langevin models the power loss will depend on the sum of the frictions on all the modes (evaluated at the appropriate vibration frequency). Thus, τ_E still scales inversely with $E^\ddagger$. In BGK models, the thermalization of even one mode will lower energy by k_BT (if $E^\ddagger/k_BT$ is greater than the number of modes, n), and hence τ_E will still be independent of $E^\ddagger$ and will be smaller by a factor of n.

The major change for the case of rapid internal energy flow is the rate of recrossings when the system is activated, k_E. This is, of course, the province of a proper RRKM calculation. A simpler RRK argument suffices to give the appropriate scaling. Assume an energy equal to the barrier $E^\ddagger$ must accumulate in the reaction coordinate in order to recross. The fraction of the $2n$-dimensional phase space satisfying this criterion is $\approx(E - E^\ddagger)^{n-1}/E^{\ddagger n-1}$, where E is the total energy in the molecule. If the excess energy is thermal, $\sim nk_BT$, we then find that the fraction is roughly $(k_BT/E^\ddagger)^{n-1}$. Since it is only for these special conditions that recrossing occurs, we would find $k_E \sim \Omega_0/2\pi(k_BT/E^\ddagger)^{n-1}$. The recrossing rate is very much smaller than for the case of no energy flow, if the barrier height is high. Thus, in the many-dimensional case, the transmission coefficient is still proportional to the external friction but it will have a much higher proportionality constant (by a factor $(E^\ddagger/k_BT)^{n-1}$). When we combine our arguments for the low- and high-friction limits, we find a nonmonotic dependence of rate on friction, as in Figure 1. The crossover from one to the other depends largely on the low-friction behavior, which, in turn, depends on details of the collisions and internal energy flow. In Kramers' original paper, his use of high barriers and the Langevin (Fokker–Planck) model led him to believe that there would always be a large plateau region where a transition-state theory is valid. Similarly, if the rapid internal energy flow ansatz is valid, there would be a large plateau, the crossover to low friction occurring only in the gas phase (because of the large prefactor $(E^\ddagger/k_BT)^{n-1}$).

Some experiments have seen the crossover in the liquid regime.[46] The exact theoretical description of these experiments is still lacking (although we are certain it will be available shortly[47]),

(40) Grote, R. F.; Hynes, J. T. *J. Chem. Phys.* **1980**, *73*, 2715.
(41) Fleming, G. R.; Courtney, S. H.; Balk, M. W. *J. Stat. Phys.* **1985**, *42*, 83.
(42) Lee, M.; Holton, G. R.; Hochstrasser, R. M. *Chem. Phys. Lett.* **1985**, *118*, 359.
(43) Pollak, E. *J. Chem. Phys.* **1986**, *85*, 865.
(44) Borkovec, M.; Berne, B. J. *J. Chem. Phys.* **1985**, *82*, 794.
(45) Nitzan, A. *J. Chem. Phys.* **1985**, *82*, 1614.
(46) Hasha, D. L.; Eguchi, T.; Jonas, J. *J. Am. Chem. Soc.* **1982**, *104*, 2290.

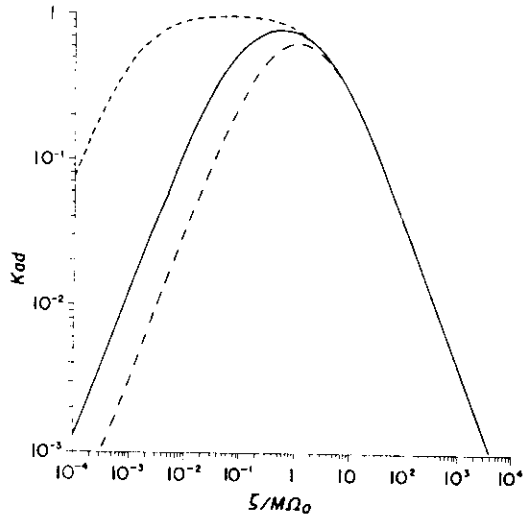

Figure 1. Plot of the "classical" adiabatic transmission coefficient k_{ad} as a function of the friction coefficient ζ in units of $M\Omega_0$. This figure is drawn by using a Padé approximation to connect the low- and high-friction limits with the TST one. A typical value is used for the activation energy ($E^{\ddagger} = 0.1$ eV) and for reorganization energy ($E_R = F^2/2M\Omega_0^2 = 0.5$ eV). The solid line is the one-dimensional (1D) Fokker–Planck result, and the lower curve (long dashes) is the 1D hard collisions (BGK) result. The top curve (short dashes) is the multidimensional nD result ($n = 3$ in this plot). The high-friction limit does not depend on the energy relaxation time but only on the velocity autocorrelation time, $\tau_v = M/\zeta$.

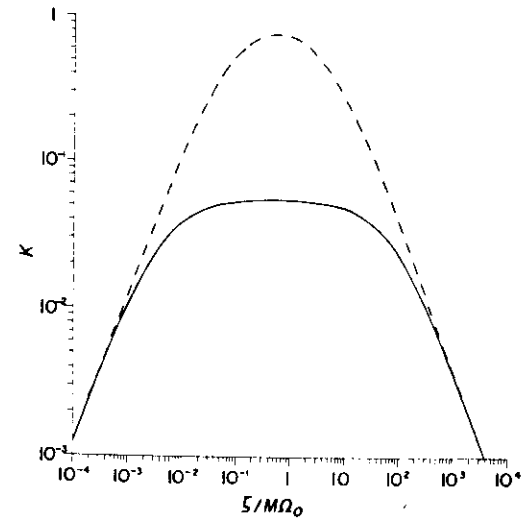

Figure 2. Plot of the "classical" transmission coefficient including the Landau–Zener probability per crossing, P_{LZ}. Here, as an example, we use $P_{LZ} = 0.03$ and a 1D Fokker–Planck dissipation mechanism is assumed. All the other parameters are defined in Figure 1. (The dashed plot is the adiabatic result of Figure 1, which is shown for comparison.) The flat plateau is the region where the rate is nonadiabatic.

but we see that the crossover in the liquid regime will be favored by low barriers for two reasons. First, the discrepancy between the limits will not be so large. Still, even for cyclohexane, it would be dramatic. The determining feature seems to be that low barriers favor poor internal energy flow. This is in keeping with the idea that regular motion dominates in low-energy systems. The low-barrier case may be quite generic for many interesting reactions, since low barriers are the rule for catalytic processes, synthetic or biological. Recently, Jonas has seen this in the rearrangement of a rhodium catalyst.[48]

II.b. Nonadiabatic Barrier Crossing in the Surface-Hopping Picture. While many chemical reactions involve motion on a single potential energy surface, some of the most important reaction processes involve motion on two different potential surfaces. Here the most dramatic deviation from the Born–Oppenheimer single-surface dynamics occurs in the region of configuration space where two (or more) potential energy surfaces nearly cross. The dynamics in the vicinity of this (avoided) crossing must be strongly quantum mechanical, but to a first approximation, the motion need not be treated quantum mechanically elsewhere. This notion is the basis of the surface-hopping picture or what we deem the "completely semiclassical" picture of nonadiabatic motion.

In this picture the system follows ordinary classical mechanics until it approaches the seam in the energy surfaces. As it crosses the seam, the probability of making an electronic-state change is computed by solving the time-dependent electronic Shcrödinger equation for a prescribed motion of the nuclei. After the system leaves the crossing region (assumed small), the decision as to which potential energy surface to follow is made probabilistically according to the probabilities computed from the electronic Schrödinger equation. Again, classical dynamics follows until the seam is reencountered. This sort of procedure has been followed for gas-phase reactions,[49] photodissociative events in condensed systems,[50] and nonadiabatic barrier crossing in the condensed phase.[51]

The one quantum aspect of the algorithm is the computation of the hopping probability. Here a reasonably reliable approximation was obtained by Landau[52] and Zener[53] for a single-crossing event. They find

$$P_{LZ} = 1 - \exp\left(-\frac{2\pi V^2}{\hbar F v_c}\right) \tag{2.3}$$

where V is the coupling between the diabatic surfaces, F is their difference in slope at the crossing, and v_c is the velocity at the crossing.

For very small V, P_{LZ} is proportional to the square of V:

$$P_{LZ} \sim \frac{2\pi V^2}{\hbar F v_c} \tag{2.4}$$

Even if only a single attempt at the crossing point is made in a typical trajectory, the transition-state theory must now be modified since it is not certain that the electronic-state change will occur. The transmission coefficient is, in that case, the velocity-weighted average of P_{LZ}. Thus, for very small V the rates go like the square of the coupling matrix element. This is the typical behavior found by perturbation theoretical Golden Rule approaches (see ref 7, for example).

As we have seen, in the condensed-phase situation, trajectories will typically cross the barrier or in this case the seam between the surfaces multiple times. Thus, the transmission coefficient is changed. Recall that the number of attempts at the seam, N_c, is roughly the inverse of the transmission coefficient for the adiabatic problem, in which the electronic-state change occurs with unit probability.

We can see the qualitative behavior using arguments of Frauenfelder and Wolynes.[4] If $P_{LZ}N_c \ll 1$, despite the number of attempts, it is unlikely that two electronic transitions occur. Thus, the probability of success on a typical path is $\sim P_{LZ}N_c$. The transmission coefficient is this probability times the same overcounting factors as in the adiabatic case, N_c^{-}. Thus, if $P_{LZ}N_c < 1$, we still find a transmission coefficient of order P_{LZ}. On the other hand, if $P_{LZ}N_c \gtrsim 1$, it is likely that several electronic-state changes have been made. The electronic state is randomized, and the probability of a change on a particular set of attempts is of order one. Still there is the overcounting due to multiple attempts, N_c^{-1}, as in the adiabatic case. So the transmission coefficient now

(47) Qualitative analytical ideas have been put forth recently: Straub, J. E.; Berne, B. J. *J. Chem. Phys.* **1986**, *85*, 2999. Barkovec, M.; Straub, J. E.; Berne, B. J. *J. Chem. Phys.* **1985**, *85*, 146. Definitive simulation work has also been done: Kuharski, R. A.; Chandler, D.; Montgomery, J. A.; Rabii, F.; Singer, S. J. *J. Phys. Chem.* **1988**, *92*, 3261.

(48) Xie, C. L.; Campbell, D.; Jonas, J. *J. Chem. Phys.*, in press.

(49) Tully, J. C.; Preston, R. K. *J. Chem. Phys.* **1971**, *55*, 262.

(50) Ali, D. P.; Miller, W. H. *J. Chem. Phys.* **1983**, *78*, 6640.

(51) Cline, R. E., Jr.; Wolynes, P. G. *J. Chem. Phys.* **1987**, *86*, 3836.

(52) Landau, L. *Sov. Phys.* **1932**, *1*, 89.

(53) Zener, C. *Proc. R. Soc. London, A* **1932**, *137*, 696.

scales just as in the adiabatic situation. Thus, the transmission coefficient varies with friction in a way as in Figure 2. It follows the adiabatic behavior in the regimes where many recrossings occur, low and high friction, but there is a wide plateau where the rate is not influenced by friction but depends on electronic coupling factors.

The qualitative argument has been confirmed (within the model) by stochastic dynamics simulation of Cline and Wolynes.[51] Straub and Berne[54] have produced an elegant semiquantitative argument that provides a convenient interpolation formula in the low-damping regime; i.e., the motion in the reactant surface is underdamped. In this limit, as shown in Figure 2, when ζ is small, N_c is large and the rate is adiabatic with a transmission coefficient $\kappa_{ad} = {}^1/_2 N_c$ proportional to ζ. The factor ${}^1/_2$ is due to the fact that there is an equal probability of decamping on reactant or product surfaces. As ζ is increased, N_c decreases until the nonadiabatic plateau is reached.

By assuming that crossings are independent (classical limit), Straub and Berne correctly computed the transmission probability on every cross as well as averaged over a distribution of values for N_c. Their final transmission coefficient is

$$\frac{1}{\kappa} = \frac{1 - P_{LZ}}{2P_{LZ}} + \frac{1}{k_{ad}} = \frac{1 - P_{LZ}}{2P_{LZ}} + 2N_c \qquad (2.5)$$

or in the case that $P_{LZ} \ll 1$

$$\frac{1}{\kappa} \sim \frac{1}{2P_{LZ}} + 2N_c \qquad (2.6)$$

In eq 2.6 the nonadiabatic transmission coefficient is $\kappa_{na} = 2P_{LZ}$. The factor 2 exists because on every trial through the crossing region there are two chances to react, the forward and reverse crossing trajectories.

As friction is increased, the motion of the reaction coordinate that was underdamped becomes overdamped. When this limit is reached, N_c starts to increase as we increase friction (N_c proportional to ζ^{-1}). Here two cases have to be discussed. In the first one, the mean free path is smaller than TST region

$$l_{TST} = k_B T/F$$

but larger than the Landau–Zener region ($l_{LZ} = V/F$). In this limit eq 2.6 is still valid, with the only difference that N_c is the number of attempts through the crossing region before the system drifts away of the TST region (see section II.a).

The second case occurs when l_{LZ} is much larger than the mean free path. In this case, called the overdamped limit because the motion is diffusive in any important length scale, the transmission coefficient is given by[5,9,10]

$$\kappa \sim \frac{4\pi^2 V^2}{\hbar}\left(\frac{M}{2\pi F^2 k_B T}\right)^{1/2} \frac{1}{1 + \frac{4\pi V^2 \zeta}{\hbar F^2}} \qquad (2.7)$$

The result above was calculated assuming harmonic surfaces for reactant and product surfaces. Equation 2.7 is the solution for the transmission coefficient in the two cases discussed above. When $P_{LZ} \ll 1$ for each particular attempt through the crossing region, details of each particular attempt are not important. The total time the system spends in the Landau–Zener region during each visit to the TST region is what counts, and this time is the same for both cases. In the adiabatic regime the transmission coefficient is basically the high-damping Kramers' one, being proportional to ζ^{-1}. This explains the high-friction behavior of Figure 2.

III. Rate Calculation in the Low Damping Regime; Quantum Effects and Adiabaticity Criteria

Up to this point the nuclear coordinate has been treated classically. In this section some quantum effects are included, and new effects like constructive and destructive interference become important. Here we discuss these effects in two contexts. First, in section III.a, they are included by using trajectory arguments which permits a direct connection to the results of section II. These arguments are inspired by the treatment of resonance and interference effects in gas-phase reactive collisions introduced by Miller and George.[61,62] Second, in section III.b, the same effects are obtained from arguments using an energy level representation which permits a direct connection to the results often obtained by using Fermi's Golden Rule.

III.a. Phases in Trajectories. In the completely semiclassical[55] treatment the transitions occur only when the reaction coordinate traverses the point at which the reactant and product diabatic surfaces cross. As already discussed (see section II.b), a reasonably good approximation for the transition probability for a single traversal is given by the Landau–Zener result

$$P_{LZ} = 1 - \exp\left(-\frac{2\pi V^2}{\hbar F v_c}\right) \sim \frac{2\pi V^2}{\hbar F v_c} \qquad (3.1)$$

We now consider the one-dimensional case discussed in section II. Reactant and product surfaces have vibrational frequency Ω_0. Also, the crossing of these two surfaces occurs at an energy E^1 (activation energy from the bottom of the donor well) larger than $k_B T$.[56] Both of these assumptions are introduced to simplify the discussion in this section, but as pointed out later in the paper, they are not necessary for most of the results presented here. In this subsection, we limit ourselves for the case $\hbar\Omega_0 < k_B T$. The other possibility, $\hbar\Omega_0 > k_B T$, is included in section III.b.

All the discussion presented in this section assumes $V \ll \hbar\Omega_0$. Without this assumption the choice of the zeroth order surfaces for reactants and products becomes questionable. Under this restriction P_{LZ} is always smaller than unity[57] (see eq 3.26). The system will typically make many traversals of the crossing point before losing $k_B T$ of energy if damping is low.[56] If τ_E is the time necessary to lose $k_B T$ of energy (see section IIa), the number of recrossings for such activated molecule is

$$N_c = \tau_E/(\Omega_0/2\pi) \qquad (3.2)$$

If the reaction coordinate is classical, N_c is all the information we need to include recrossing effects. This is not sufficient if quantum effects are important. Here we have to introduce the concept of coherence time, t_{coh}. This is the time for which motion in the reactant and product wells maintains a constant phase relation.

If the particle relaxes out of the transition-state region (reactive region), the phase between reactant and product is automatically destroyed and the relaxation time out of the transition-state region cannot be shorter then the coherence time, i.e., $\tau_E \geq t_{coh}$. In most of the cases $\tau_E \gg t_{coh}$.

In the same way we defined N_c, we can now define the number of coherent crosses as

$$N_{coh} = t_{coh}(\Omega_0/2\pi) \qquad (3.3)$$

As an example of the difference between these two times, we discuss the spin-boson Hamiltonian for chemical reactions.[5,10,51] In this case, since the environment and the reaction coordinate are harmonic, the only way that the phase difference between these wells can be destroyed is by relaxation (either in the reactant or

(54) Straub, J. E.; Berne, B. J. *J. Chem. Phys.* 1987, *87*, 6111.

(55) As always, the word "semiclassical" can take on many meanings. By "completely semiclassical" we mean treatments that treat the nuclei moving classically except at curve crossing where the electronic state is chosen probabilistically using probabilities found by integrating the electronic Schrödinger equation for the prescribed nuclear motion. This is the surface-hopping algorithm.

(56) The reactant and product surfaces are assumed to be in the strong coupling limit; i.e., if damping is small, the reorganization energy ($F^2/2M\Omega_0^2$) has to be larger than $\hbar\Omega_0$. Quantum mechanically speaking, this means wek overlap between reactant and product eigenfunctions. Otherwise, i.e., in the weak coupling limit, there is no need to activate the system to energies of order E^1 before the reaction can occur.

(57) In this regime, complexity is removed—the motion is diabatic or adiabatic surfaces need not be distinguished. If P_{LZ} is of order one, this distinction is more crucial, but we believe the arguments have qualitative validity since the rate then is crucially adiabatic.

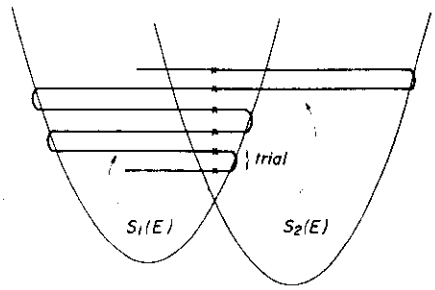

Figure 3. Schematic representation of how phases are added in eq 3.5. Here we show how we pick up a phase $S_1(E)/\hbar$ moving in the reactant surface and a phase $S_2(E)$ moving in the product surface. We also show what we call a trial that is composed by the two crossings because most trajectories going through the transition state cross the cusp twice. The decrease in energy of the trajectory as it crosses the wells has, unfortunately, been exaggerated for visual clarity.

in the product). But to destroy coherence it is enough to lose or gain only $\hbar\Omega_0$ (not k_BT). Therefore, for this particular case[14]

$$\tau_E \sim \frac{k_BT}{E^\ddagger}\frac{M}{\zeta} \tag{3.4a}$$

and

$$t_{coh} \sim \frac{(\hbar\Omega_0)^2}{E^\ddagger k_BT}\frac{M}{\zeta} \tag{3.4b}$$

The presence of significant anharmonicity and/or "random" fluctuations to the frequencies of motion are able to destroy coherence before any relaxation takes place. These effects basically do not affect τ_E, but they can strongly reduce t_{coh}. If the notation used in magnetic resonance and nonlinear spectroscopy is loosely used, t_{coh} is basically the well-known time T_2,[58] the time that takes for reactant and product states to lose phase coherence between them. This may occur, due to the mechanisms described above, in times much shorter than the time necessary to lose or gain $\hbar\Omega_0$ (eq 3.4b), which would be associated in the spectroscopy literature with T_1. Therefore, if relaxation is the only process available to destroy coherence, $t_{coh} \sim T_2 \sim T_1$. Otherwise, if the other effects dominate, $t_{coh} \sim T_2 \ll T_1$.

When the trajectory is incident on the crossing region with energy E, initially it either may make a transition with probability P_{LZ} or may not with probability $1 - P_{LZ}$. The reader will find it convenient to refer to Figure 3 during the following argument. The probability amplitude for the transition is hence $P_{LZ}^{1/2}\exp(i\phi)$ where ϕ is the Stuckelberg phase.[59] Most trajectories going through the transition state cross the cusp twice. They pick up a probability amplitude A_{LZ}, such that $|A_{LZ}|^2 = 2P_{LZ}$.[60] If it goes to the product during this crossing trial (two crosses), it will pick up a phase $\exp\{iS_2(E)/\hbar\}$ while traveling across the product well. The action S_2 is given by $S_2(E) = 2\pi\Omega_0^{-1}(E - E_p) + \hbar\pi/2$ where E_p is the depth of the product well. It contains a correction for the Maslov index at the turning point. On the other hand, if it fails to cross, it will pick up a phase $\exp\{iS_1(E)/\hbar\}$ where $S_1(E) = 2\pi\Omega_0^{-1}(E - E_r) + \hbar\pi/2$ and the reactant well depth is E_r.[61,62] If we consider the amplitude for the paths involving only one electronic state change during roughly N_{coh} trials, we find

$$A \sim A_{LZ}\sum_{N=0}^{N_{coh}^{-1}} e^{(i/\hbar)S_1(E)N}e^{(i/\hbar)S_2(E)(N_{coh}-N)}$$

$$\sim A_{LZ}e^{(i/\hbar)S_2(E)N_{coh}}\sum_{N=0}^{\infty} e^{-N/(N_{coh}-1)}\left(e^{(i/\hbar)2\pi\Omega_0^{-1}\Delta E}\right)^N \tag{3.5}$$

where $\Delta E = E_r - E_p$. In this expression N is the number of attempts before a transition is made. In the last formula we have introduced a more realistic smooth cutoff in the number of traversals (tantamount to a "Poisson distribution") rather than the sharp one used in the verbal discussion. Before evaluating this sum, we note that since $\exp(2\pi i) = 1$ the exothermicity ΔE is evaluated mod $\hbar\Omega_0$ giving $\Delta E \to (E_r - E_p)_{\text{mod }\hbar\Omega_0} = \delta E$. Thus, sum (3.5) gives

$$A \sim A_{LZ}\exp\left\{\frac{i}{\hbar}S_2(E)N_{coh}\right\}\frac{1}{1 - \exp\left(-\frac{1}{N_{coh}-1} + \frac{2\pi i\delta E}{\hbar\Omega_0}\right)}$$

$$\sim A_{LZ}\exp\left\{\frac{i}{\hbar}S_2(E)N_{coh}\right\}\frac{1}{\frac{1}{N_{coh}-1} - \frac{2\pi i\delta E}{\hbar\Omega_0}} \tag{3.6}$$

The latter expression is valid for small energy mismatching and large coherence times ($N_{coh} \gg 1$ and $\delta E \ll \hbar\Omega_0$).

The probability is the square magnitude of A:

$$P_{coh} \sim 2P_{LZ}\frac{1}{1 + \exp\left\{-\frac{2}{N_{coh}-1}\right\} - 2\exp\left\{-\frac{1}{N_{coh}}\right\}\cos\left(\frac{2\pi\delta E}{\hbar\Omega_0}\right)}$$

$$\approx \frac{2P_{LZ}}{\frac{1}{(N_{coh}-1)^2} + \frac{(2\pi\delta E)^2}{(\hbar\Omega_0)^2}} \tag{3.7}$$

again the latter for N_c large and δE small.

If there is exact resonance between the wells, there is a great deal of constructive interference and one obtains $P_{coh} = P_{coh}^{res} = 2P_{LZ}N_{coh}^2$. On the other hand, if there is exact antiresonance ($\delta E = \hbar\Omega_0/2$), there is a modest amount of destructive interference

$$P_{coh} = \frac{2P_{LZ}}{1 + \exp\left\{-\frac{2}{N_{coh}-1}\right\} + 2\exp\left\{-\frac{1}{N_{coh}-1}\right\}}$$

$$\to P_{coh}^{anti} = \frac{P_{LZ}}{2} \quad \text{for large } N_{coh} \tag{3.8}$$

In both cases if there is no recrossing during a phase relaxation time, $P_{coh} = 2P_{LZ}$. Also, since $k_BT > \hbar\Omega_0$, the average crossing velocity we should use in P_{LZ} is v_c of the order $(k_BT/M)^{1/2}$.

Now we must also consider the probability arising from the incoherent passes across the cusp. We use the notation N_{inc} to denote the number of incoherent attempts, $N_{inc} = N_c/N_{coh}$, if there are many crossings.

In the particular case of the spin-boson Hamiltonian (see eq 3.4), the number of independent attempts is

$$N_{inc} = \frac{N_c}{N_{coh}} = \frac{\tau_E}{\tau_{coh}} \approx \left(\frac{k_BT}{\hbar\Omega_0}\right)^2 \tag{3.9}$$

If P_{coh} is of order one, we get for the transmission coefficient $\kappa = {}^1/_2N_c$, and this is the usual Kramers low-damping result proportional to the collision frequency. This limit is carefully addressed in section III.b. If P_{coh} is small, i.e., $P_{coh} \ll 1$, the sequence of attempts has a probability of leading to the product

$$P_c \approx P_{coh}\frac{N_c}{N_{coh}} \tag{3.10}$$

(58) Slichter, C. P. *Principles of Magnetic Resonance*; Harper and Row: New York, 1963.

(59) Stueckelberg, E. G. C. *Helv. Phys. Acta* **1932**, *5*, 369.

(60) Since double crossing occurs, the forward and backward cross lead to a probability amplitude $A_{LZ} = (P_{LZ}^{1/2} + e^{i\delta}P_{LZ}^{1/2})\exp(i\phi)$. δ is the phase accumulated between these two crosses. This leads to $|A_{LZ}|^2 = 2P_{LZ}(1 + \cos\delta)$. Because $k_BT > \hbar\Omega_0$, when we average over all possible energies k_BT of the crossing region $(\cos\delta) = 0$. Therefore, $|A_{LZ}|^2 \sim 2P_{LZ}$.

(61) Miller, W. H. *J. Chem. Phys.* **1978**, *68*, 4431.

(62) Miller, W. H.; George, T. F. *J. Chem. Phys.* **1972**, *56*, 5637.

If this reaches one in magnitude, then $P_c \approx {}^1/_2$, and again we obtain the usual classical low-damping Kramers result, i.e., $\kappa = {}^1/_2 N_c$. On the other hand, if P_c calculated as above is small, the transmission coefficient is

$$\kappa = \frac{P_c}{N_c} = \frac{P_{coh}}{N_{coh}} \tag{3.11}$$

This is the nonadiabatic limit, which gives a rate proportional to V^2.

The correct interpolations between these two limits can be obtained by doing the probabilistic counting à la Straub and Berne[54] (see section II.b for details) by substituting P_{LZ} of the "classical" equation by $P_{coh}/2$ and N by N_c/N_{coh}. The reason for these substitutions is because in the classical case we had independent crosses and here we have independent trials per coherence time. The factor 2 dividing P_{coh} is because we have two crossings per trial in the classical case. Thus

$$\frac{1}{P_c} = \frac{1}{P_{coh}(N_c/N_{coh})} + 2 \tag{3.12}$$

This leads to a transmission coefficient

$$\frac{1}{\kappa} = \frac{N_c}{P_c} = 2N_c\left(1 + \frac{1}{2(N_c/N_{coh})P_{coh}}\right) \tag{3.13a}$$

or

$$\frac{1}{\kappa} = N_{coh}\left(2\frac{N_c}{N_{coh}} + \frac{1}{P_{coh}}\right) \tag{3.13b}$$

The term in parentheses is exactly the Straub and Berne expression given in the last section by doing the substitution described before. The factor N_{coh} multiplies everything because now we have N_{coh} double crosses per trials instead of only one double cross as in the classical case.

Conditions for adiabaticity and nonadiabatricity in the rate appear naturally from eq 3.13. Also, N_{coh} approaches one as $P_{coh} \to 2P_{LZ}$ because crosses become independent, and our quantum result becomes the classical result described in section II.

In Figure 2, we show the rate dependence on friction assuming we have Fokker–Planck dissipation (exactly as in the spin-boson case). As we increase ζ (friction coefficient), the rate is linear on ζ until it reaches the nonadiabatic plateau ($4P_{LZ}N_c > 1$). This is equivalent to saying the rate is proportional to $1/N_c$ (see eq 3.4); that is, it is constant for some values of ζ, until it reaches the adiabatic diffusive limit and it becomes proportional to $1/\zeta$. Here we are only interested in corrections to the low-damping regime, i.e., the region proportional to ζ and the plateau one.

Now we discuss two possible situations: the first one is if N_{coh} becomes one at values of the friction lower than where the classical plateau occurs. The condition found for adiabaticity from eq 3.13b is $X = 2P_{coh}N_c/N_{coh>1}$. When the two wells are resonant, this gives a much stronger condition on the nonadiabatic result since

$$X_{res} = 4P_{LZ}N_cN_{coh} > 4P_{LZ}N_c = X_{cl} \tag{3.14}$$

Therefore, in this situation the quantum result follows the classical adiabatic rate for low friction. However, in the antiresonant case, we have

$$X_{antires} = P_{LZ}\frac{N_c}{N_{coh}} < 4P_{LZ}N_c = X_{cl} \tag{3.15}$$

Thus, for large values of N_{coh}, $X_{antires} \ll$ (3.15). The rate is still nonadiabatic in contradistinction to the usual classical crossing argument. The transmission coefficient is

$$\kappa \sim \frac{P_{LZ}}{2N_{coh}} \propto \frac{V^2}{t_{coh}} \tag{3.16}$$

In the Fokker–Planck or spin-boson case it still is proportional to ζ but with a completely different slope. In a more general case it is proportional to t_{coh}^{-1}. As N_{coh} becomes one, it becomes the adiabatic classical result. This N_{coh} limit, varying from resonant to nonresonant case, is shown in Figure 4.

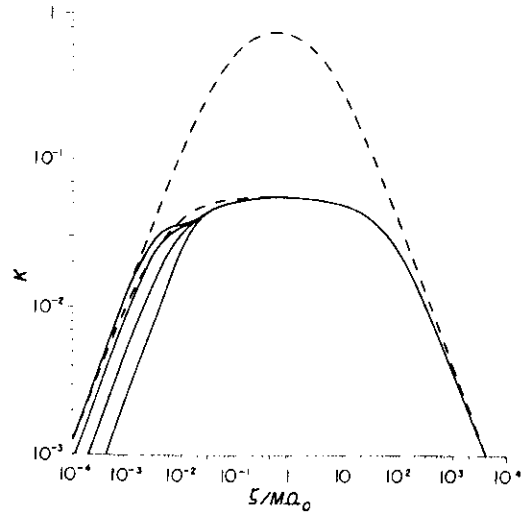

Figure 4. Plot of the "quantum" transmission coefficient as a function of $\zeta/M\Omega_0$. The top dashed curve is the "classical" adiabatic transmission coefficient including Landau–Zener corrections, and the lower one is the total "classical" transmission coefficient. (Both of these curves are given in Figure 2, where most of the parameters used in this figure are defined.) N_{coh} is assumed to be a function of ζ^{-1} and becomes unity for a given value of the friction coefficient that we call ζ^*. In this plot we assume that N_{coh} becomes one before the "classical" nonadiabatic region (plateau) is reached. For example, we chose $\zeta^* = 0.005M\Omega_0$. The "quantum" plots are given by solid lines that use, from left to right, $\delta E/\hbar\Omega_0 = 0.0$, 0.1, 0.2, and 0.5.

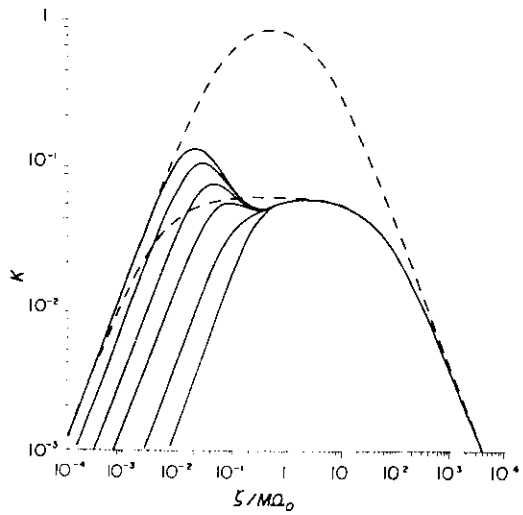

Figure 5. Same as Figure 4 but with ζ^* in the "classical" nonadiabatic region. For example, we chose $\zeta^* = 0.1M\Omega_0$. The "quantum" plots are given by solid lines that use, from left to right, $\delta E/\hbar\Omega_0 = 0.0$, 0.03, 0.06, 0.1, 0.2, and 0.5.

If N_{coh} becomes one in the plateau region of Figure 2, the behavior is different. The off-resonance case has basically the same behavior discussed before with the difference that it reaches the classical result only in the plateau region when $N_{coh} \sim 1$. The resonance case is the interesting one. From eq 3.14 we notice it agrees with the classical result up to the plateau region. After that, it continues adiabatic until $4P_{LZ}N_{coh}N_c \sim 1$. After that it drops in value until it reaches the classical behavior for $N_{coh} \sim 1$. This limit is shown in Figure 5. Notice the characteristic resonant peak behavior which is seen here as the friction is varied.

To conclude this subsection, we write the final expression for the rate in the nonadiabatic limit, i.e., $P_c \ll 1$. In this limit

$$\kappa \sim \frac{P_{coh}}{N_{coh}}k_{TST} = \frac{P_{coh}}{N_{coh}}\frac{\Omega_0}{2\pi}\exp\left(-\frac{E^\ddagger}{k_BT}\right) \tag{3.17a}$$

or

$$k = \frac{P_{LZ}(\hbar\Omega_0)^2}{2\pi^2\hbar}\,\frac{(\hbar/t_{coh})}{(\hbar/t_{coh})^2 + \delta E^2}\exp\left(-\frac{E^\ddagger}{k_BT}\right) \qquad (3.17b)$$

This is the rate that will be compared to the Fermi Golden Rule result (see ref 8 and 26, for example), which is one of the main points of the following subsection.

III.b. Energy Levels and Fermi Golden Rule. Now we use a different approach to calculate the reaction rate, assuming that the reactant and product surfaces are harmonic oscillators weakly damped. We label the energy levels in the reactant which are equally spaced by $\hbar\Omega_0$ by n_A and the ones in the product by m_B.

Since $k_BT > \hbar\Omega_0$, the rate is dominated by levels near the crossing region. If we get a level in this region n_A, the transitions to the acceptor are dominated by a level m_B which is the one closest in energy. Since $\delta E = E_{n_A} - E_{m_B} = (E_r - E_p)_{\text{mod }\hbar\Omega_0}$, the rate k_{n_A,m_B} calculated by the Fermi Golden Rule (perturbation in V) is

$$k_{n_A,m_B} = \frac{2\pi}{\hbar}\int dE\ \rho_{n_A}(E)|V(n_A|m_B)|^2\,\rho_{m_B}(E) \qquad (3.18)$$

where

$$\rho_i = \frac{1}{\pi}\,\frac{(\hbar\Gamma_i)}{(E - E_i)^2 + (\hbar\Gamma_i)^2} \qquad (3.19)$$

is the density of states around level i. If we perform this integral

$$k_{n_A,m_B} = \frac{2\pi}{\hbar}|V_{n_A,m_B}|^2\frac{1}{\pi}\,\frac{\hbar(\Gamma_{n_A} + \Gamma_{m_B})}{(\delta E)^2 + [\hbar(\Gamma_{n_A} + \Gamma_{m_B})]^2} \qquad (3.20)$$

where

$$V_{n_A,m_B} = V(n_A|m_B) \qquad (3.21)$$

Here Γ_i is the width of level i. In a more correct way each should be associated with the coherence time between levels. Therefore, from now on we use t_{coh}^{-1} (defined in section III.a) instead of $\Gamma_{n_A} + \Gamma_{m_B}$. ($\Gamma_{n_A} + \Gamma_{m_B}$ is the relaxation frequency associated with gaining or losing a phonon of energy $\hbar\Omega_0$. Therefore, they are associated with $1/T_1$ and the frequency we need here is $1/T_2$.)

If equilibration of the reactant states is fast enough compared to the rates k_{n_A,m_B} for the pair levels which dominate the rate (levels k_BT around the crossing point[56]), the final rate is obtained, summing the contribution of all levels around the crossing region,

$$k \sim \sum_{n_A} k_{n_A,m_B}\rho(n_A,T) \qquad (3.22)$$

where m_B is the closest level in energy to n_A and $\rho(n_A,T)$ is the thermal equilibrium distribution of the reactant states.

Here we include some comments about relaxation. Notice that in eq 3.22 we are calculating a rate as an average of pair rates. So, if equilibration is not fast enough, the number of reactants in this reactive region is depleted faster than new reactants are able to come to this region. In this case eq 3.22 breaks down.

The question now is how to compare eq 3.22 with eq 3.17. This can be done by using the semiclassical estimate of $\langle n_A|m_B\rangle$.[63] Because we are considering states with energy k_BT above the crossing region $E_{n_A} \approx E_{m_B} > V_c$ (V_c is the crossing region energy, $V_c = E^\ddagger + E_r$), then

$$\langle n_A|m_B\rangle = \int\frac{dx}{N^2}\,\frac{1}{(p_A(x))^{1/2}}\,\frac{1}{(p_B(x))^{1/2}}\exp\left[\frac{i}{\hbar}\int^x(p_A(x') - p_B(x')\,dx'\right] \qquad (3.23)$$

where

$$p_A(x) = [2M(e - V_r(x))]^{1/2} \qquad (3.24a)$$

$$p_B(x) = [2M(E - V_p(x))]^{1/2} \qquad (3.24b)$$

and N is the normalization constant. Calculating this integral (3.23) by noticing that the stationary-phase value occurs at the crossing point, we get

$$|\langle n_A|m_B\rangle|^2 \sim \frac{2\hbar}{\pi}\,\frac{\Omega_o^2}{v_cF} \qquad (3.25)$$

where $^1/_2Mv_c^2 = E - V_c$. Thus

$$P_{LZ} \sim \pi^2\frac{V^2}{(\hbar\Omega_0)^2}|\langle n_A|m_B\rangle|^2 \qquad (3.26)$$

Recall that levels that dominate the rate are about k_BT above the crossing point, giving this an average value for the kinetic energy in the crossing point.

Using eq 3.20, 3.22, and 3.26, we obtain for the rate

$$k \sim \sum_{n_A}\frac{2\pi}{\hbar}\,\frac{(\hbar\Omega_0)^2}{\pi^2}\,\frac{1}{\pi}\,\frac{\hbar/t_{coh}}{\delta E^2 + (\hbar/t_{coh})^2}\,P_{LZ}\rho(n_A,T) \qquad (3.27)$$

where, because $k_BT > \hbar\Omega_0$, we do a continuum approximation to evaluate $\langle 1/v_c\rangle$. So

$$\sum_{n_A}P_{LZ}\rho(n_A,T) = \frac{2\pi}{\hbar}\,\frac{V^2}{F}\int_{E^\ddagger}^{\infty}\frac{1}{v_c}\rho_A(E,T)\,dE = \frac{2\pi V^2}{\hbar F}\left(\frac{\pi M}{2k_BT}\right)^{1/2}\exp\left(-\frac{E^\ddagger}{k_BT}\right) \qquad (3.28)$$

The rate becomes

$$k \sim \frac{2P_{LZ}(\hbar\Omega_0^2)}{\pi^2\hbar}\,\frac{\hbar/t_{coh}}{\delta E^2 + (\hbar/t_{coh})^2}\exp\left(-\frac{E^\ddagger}{k_BT}\right) \qquad (3.29)$$

where we use $v_c = (2k_BT/\pi M)^{1/2}$ for the velocity in P_{LZ}. Coherence times for all levels in an interval k_BT around the crossing point are not necessarily the same but are very similar. In the spin-boson Hamiltonian (Fokker–Planck dissipation) this is easily noticed since $k_BT \ll E^\ddagger$ (see eq 3.4b and ref 14). Equations 3.29 and 3.17 are basically the same. They differ by a factor of 4 which is irrelevant, and it is due to approximations in eq 3.6–3.8, as well as in the calculation of eq 3.26.

In the language of levels the Golden Rule formula can break down for two reasons, in a way analogous to the trajectory arguments presented in section III.a. The first reason is that the expression given for k_{n_A,m_B} given by eq 3.20 has to be valid. This will be true only when t_{coh} is fast enough to destroy coherence between levels n_A and m_B. In the trajectory argument this is equivalent to say $P_{coh} \ll 1$, that is, exactly the same condition that $k_{n_A,m_B} \ll t_{coh}^{-1}$ (k_{n_A,m_B} given by eq 3.20).

The second reason is equilibration, and that is controlled by energy flow between reaction coordinate and environment, i.e., the time τ_E. In the trajectory argument this means $P_c \ll 1$. In this energy-state argument the equivalent condition is that the system has to relax out of the reactive region faster than the reaction takes place, i.e., $k_{n_A,m_B} \ll \tau_E^{-1}$ (k_{n_A,m_B} given by eq 3.20). Assuming the first condition is satisfied ($k_{n_A,m_B} \ll T_{coh}^{-1}$), the condition above can be obtained in a more elegant way. This is done by writing a master equation[27,28,64] including motion between reactant levels and product levels (vertical transition) due to the interaction between reaction coordinate and environment as well as horizontal transitions (between reactant and product, or vice versa) with rates k_{n_A,m_B}. The solution of this master equation would lead to the same condition described above for the Golden Rule rate. Also, it would give the interpolation between the adiabatic and nonadiabatic limits for the rate with a final expression which would be basically the one given by eq 3.13.

In this energy level description, we can now analyze more carefully the limit when "P_{coh}" becomes larger than unity. Since $P_{LZ} \ll 1$, this occurs only in resonant cases when $P_{LZ}N_{coh}^2 > 1$. In this limit, the system should oscillate between pair of levels (n_B, m_B) before losing coherence. This is the quantum beat

(63) See for example: Merzbacher, E. *Quantum Mechanics*; Wiley: New York, 1970; Chapter 7.

(64) Cribb, P. H.; Nordholm, S.; Hush, N. S. *Chem. Phys.* 1978, 29, 43.

regime.[65] The system oscillates between reactant and product states in times much shorter than t_{coh} so that when coherence is destroyed it may be found in the reactant and product state with roughly equal probability when the levels are resonant. This is a tricky regime and at some point in the future should be investigated more thoroughly.

Now that we have considered the case $\hbar\Omega_0 < k_BT$, we must address the situation $\hbar\Omega_0 > k_BT$. In this regime, the lowest state in the reactant dominates the rate. An interesting way of noticing this is by calculating the mean-square displacement of the reaction coordinate, due to the fact that the rate is proportional to $\exp(-E^\ddagger/M\Omega_0^2\mu^2)$.[56] In the harmonic case $\mu^2 = k_BT/M\Omega_0^2$ if $k_BT \gg \hbar\Omega_0$, and $\mu^2 = \hbar/2M\Omega_0$ if $k_BT \ll \hbar\Omega_0$, i.e.; only the reactant ground-state contributes to it. In more general surfaces competition between tunneling and thermal activation is not so simple. In this limit, the reaction rate is

$$k \sim k_{0,m_B^0} \sim \frac{2\pi}{\hbar}V^2|\langle 0|m_B^0\rangle|^2\frac{1}{\pi}\frac{\hbar/t_{coh}}{\delta E^2 + (\hbar/t_{coh})^2} \qquad (3.30)$$

where $|m_B^0\rangle$ is the level in the product that is closest in energy to the ground state of the reactant. The overalp $|\langle 0|m_B^0\rangle|^2$ can be calculated similarly to eq 3.23. The difference is that the ground-state energy E_0 is below V_c, and therefore, there are tunneling trajectories. The result obtained is basically the same one given by eq 3.25

$$|\langle 0|m_B^0\rangle|^2 \sum \frac{2\hbar}{\pi}\frac{\Omega_0^2}{v_cF} \qquad (3.31)$$

with the difference that here v_c is the imaginary velocity given by $^1/_2Mv_c^2 = V_c - E_0$.

There are two particular points associated with this limit. If $E_r - E_p > \hbar\Omega_0$, i.e., reaction is exothermic, the relaxation time τ_E is now the time it takes for the product state to lose $\hbar\Omega_0$ of energy, because this is the minimum meaningful energy loss. The second point we discuss is when the reaction has no energy gap, i.e., $E_r = E_p$. In this situation there is no state that the "activated molecule" can relax to. Reaction is "occurring" between two ground states. Therefore, the definition of a rate becomes questionable.

To conclude this section, we comment about another possible new quantum effect that can occur for $k_BT > \hbar\Omega_0$. In this regime we stated that the rate was dominated by states around the crossing region. This may not be true in some cases. Using eq 3.26, we can calculate P_c for every reactant–product pair of levels. The interesting effect occurs if P_c becomes of order unity for levels below the crossing region. (This may occur even in the strong coupling limit assumed here.[56]) In this limit the rate becomes adiabatic with an activation barrier smaller than $E^\ddagger$. Here quantum effects change not only the transmission coefficient but also the activation energy of the reaction.

IV. Discussion and Speculation

In this paper we have tried to outline the connection between quantum and classical pictures of barrier crossing, especially in the case where surface crossing is involved. The interplay between dephasing and energy loss in determining the importance of resonance effects emerges clearly in this simple picture of a simple model. There are immediately then two questions: What are the prospects for devising simple experiments to test and illustrate these effects? Do these effects play any role in more complicated (multimode) situations? We will give some speculative answers to these questions.

The picture we have pursued is largely one-dimensional—a single mode of motion is taken to be the reaction coordinate. Also in this model, the interesting quantum effects occur when this mode of motion is highly underdamped. In electron-transfer reactions this situation will be most closely imitated by reactions that are largely inner sphere dominated. Unfortunately, this will usually put us in the strong quantum limit ($\hbar\Omega_0 > k_BT$) so the energy relaxation effects are minimal. Perhaps electron transfer in some organic or biological systems may give the possibility of the region where $k_BT > \hbar\Omega_0$.

The resonance and dephasing effects are, however, accessible. The most complete studies (could) utilize spectroscopic measurements of dephasing times[66] along with pressure tuning[67] to pin down these effects. A candidate experimental system is then an inner-sphere reaction going on in a crystalline matrix.

Generally, then we will have a multidimensional system in which no single mode is the reaction coordinate. The quantum effects may still play a role, although indirectly. In one possible realization, the additional (to the underdamped) reaction modes are slowly fluctuating or diffusing in a nearly classical way. These fluctuations can act to "tune" the resonances. If the inner-sphere resonances are sufficiently strong (T_2 long), the electronic transition itself would no longer be rate limiting. The "tuning" dynamics would then be crucial, and one would expect adiabatic results in the sense of being insensitive to electronic matrix element.

A more problematic (but interesting) situation arises when the strongly coupled reaction modes are comparable in time scales and are underdamped. In this case, even when there are no quantum effects, we have the issue of energy flow between modes and its effect on recrossing rates (see section II). If the quantum interference effects are included, one must take into account the phases of crossing trajectories. In a chaotic system these are apt to be random. In the nonadiabatic regime there should, therefore, be little change in the rate since in sums of squared matrix elements the phases will cancel. It is conceivable, however, there will be effects on the adiabaticity criterion. For *some* crossing energies the random phases will happen to add up in phase. For those trajectories (or levels) the rate will reach its maximum value. The rapid rate of reaction from these resonant levels means they can be such effective sinks of probability that the electronic-state change is no longer rate limiting. Instead, incoherent fluctuations involving energy dissipation will scan these trajectories and the rate may then become, at least partially, adiabatic dependent on the energy dissipation rate. Certainly, both of these multidimensional situations merit further study.

To conclude, we comment about the validity of semiclassical approximations to calculate reaction rates. As extensively discussed in section III, phase effects are important only if $N_{coh} > 1$. When N_{coh} becomes one, semiclassical calculations of the rate become valid. In the case of the spin-boson Hamiltonian (harmonic reaction coordinate and bath), t_{coh} (or T_2) is controlled by relaxation processes and, therefore, it has a tendency to overestimate quantum effects. In real systems T_2 may be much shorter, making the semiclassical calculations good approximations under much weaker conditions than expected from the spin-boson Hamiltonian.

Acknowledgment. We thank J. J. Hopfield and M. Newton for helpful discussions. We are both grateful to the Institute for Theoretical Physics for its kind hospitality. P. G. Wolynes thanks the Institute for Molecular Science for their hospitality as well. This work was supported by the National Science Foundation under Grants PCM-8406049 and CHE-8418619. Work in Santa Barbara was partially supported by NSF Grant PHY-8217853 supplemented by funds from the National Aeronautics and Space Administration. J. N. Onuchic also received partial support from the Brazilian Agencies CNp_q and FINEP and from the Department of Energy's Energy Conservation and Utilization Technologies Program (ECUT) during a visit to the Jet Propulsion Laboratory, California Institute of Technology. P. G. Wolynes also thanks the J. S. Guggenheim Foundation for their generous support.

(65) A ground-breaking study in this regime was carried out by Friesner and Wertheimer (ref 25b). They discussed, however, only a model for electron transfer in the photosynthetic reaction center which appears to be activationless.

(66) Dlott, D. D. *Annu. Rev. Phys. Chem.* **1986**, *37*, 157.
(67) Drickamer, H. G. *Acc. Chem. Res.* **1986**, *19*, 329.